https://doi.org/10.53964/jmab.2026001

https://www.innovationforever.com

Journal of
Modern Agriculture and Biotechnology

ISSN 2788-810X (Online)

Open Access

Research Article

In vitro spectrophotometric method for determination of various mycotoxins and their *in Silico* Assessment Based on Cholinesterase Inhibitions through the Molecular Docking Approach

Rashid Akhundov[1*]

[1]Lomonosov Moscow State University, Chemistry Department, Moscow, Russia

[*]**Correspondence to: Rashid Akhundov,** Master of Chemistry, Chemistry Department, Leninskie Gory 1/ 3, Moscow Russia; Email: axundovrashid@gmail.com, axundovrashid@protonmail.com

Received: October 29, 2025 **Revised:** November 19, 2025 **Accepted:** January 5, 2026 **Published:** March 3, 2026

Abstract

Objective: This article discusses approaches to the *in vitro* spectrophotometric determination of various mycotoxins and their *in silico* assessment using the molecular docking method based on cholinesterase inhibition effects.

Methods: The following tools were used in this study: the Ellman spectrophotometric method for assessing the formation of thiocholine, a product of enzymatic hydrolysis of acetylthiocholine and butyrylthiocholine in the presence of enzymes, respectively; the ChemBio3D Ultra software package; the AutoDock Vina 1.1.2 docking softvare; and the PyMol visualization tool.

Results: The type and degree of enzyme inhibition for mycotoxin zearalenone (ZEN), depending on incubation time and Acetylcholinesterase (AchE) enzyme concentration, was determined, showing the competitive type of inhibition. The inhibition constant is 15±4μmol/l. K_m, V_{max}/E_0 and $V_{max}/(E_0 \cdot Km)$ were established for the enzymatic hydrolysis of acetylthiocholine and butyrylthiocholine by AchE and Butyrylcholinesterase (BchE) enzymes, respectively. For AchE: K_m=98±23μmol/l, V_{max}/E_0=316±26min^{-1}, $V_{max}/(E_0 \cdot K)$=3.22±1.02 l/μmol•min. For BchE: K_m=319±35μmol/l, V_{max}/E_0=8.3±0.2 min^{-1}, $V_{max}/(E_0 \cdot K_m)$=0.027±0.003 l/μmol•min. For ZEN, the concentration range is 0.5-50 mg/l, sterigmatocystin (STC) - 0.25-0.8 mg/l, deoxynivalenol (DON) - 1.25-25 mg/l, ochratoxin A (OTA) - 2.5-10 mg/l. Molecular docking analysis of four mycotoxins, specific substrates, and co-crystallized ligand inhibitors was performed, affinities (binding energies, kcal/mol) for those compounds were found.

Conclusion:. A method for determining mycotoxins using biosensors based on AchE and BchE was developed. The corresponding calibration graphs and meaningful inhibitory effects of four mycotoxins on AchE and BchE enzyme activity were constructed.

Keywords: Cholinesterase, mycotoxins, inhibitor, biosensor, molecular docking, Acetylcholinesterase, Butyrylcholinesterase, zearalenone, ochratoxin A, sterigmatocystin, deoxynivalenol, Molecular Visualization and Graphics System

Citation: Akhundov R. *In vitro* spectrophotometric method for determination of various mycotoxins and their *in Silico* Assessment Based on Cholinesterase Inhibitions through the Molecular Docking Approach. *J Mod Agric Biotechnol*, 2026; 5: 1. DOI: 10.53964/jmab.2026001.

https://doi.org/10.53964/jmab.2026001

1 INTRODUCTION

Cholinesterase-based biosensors have been widely used for the analysis of various toxic compounds, including mycotoxins. First of all, enzyme inhibition-based biosensors are useful analytical tools for rapid screening of inhibitors. Cholinesterases (ChE) are a family of enzymes that catalyze the hydrolysis of choline esters, some of which serve as neurotransmitters. Reversible ligands, such as tacrine and donepezil, which interact with the enzyme near its catalytic center, do not form a covalent complex but rather interact with the enzyme via weak bonds similar to those used for substrate binding. These bonds have been shown to be easily broken and instantly re-formed. As a result, reversible inhibitors are effective immediately but do not block the enzyme permanently. The durations of action of these agents are very short (only about minutes)[1,2]. Biosensors cannot be compared with analytical methods such as mass spectrometry or chromatography for the neurotoxic compounds being studied, although they offer advantages such as ease of use and low cost. On the other hand, it should be noted that many scientists view ChE as a model for the development of new biosensors, nanotechnologies, and immobilization methods.

Feed typically contains several types of mycotoxins, which poses an additional risk, as their interactions can lead to a two-way toxicity boost. A particular danger lies in the fact that mycotoxins tend to accumulate in body tissues, so even low concentrations of these substances in food and feed should be avoided. According to generally accepted standards, the content of deoxynivalenol (DON) in feed should not exceed 0.75-1mg/kg, ochratoxin A (OTA) - 0.01mg/kg, zearalenone (ZEN)- 1.0mg/kg, and sterigmatocystin (STC)- 0.05-0.1mg/kg. To further characterize the risk of low contamination levels, a literature search was performed to identify published studies on the effects of DON, ZEN at concentrations at or below the European Union guidance values applicable for aquaculture feed - DON: 5mg/kg; ZEN: 2mg/kg[3].

Emerging mycotoxins, including nivalenol, enniatins, beauvericin, diacetoxyscirpenol, fusaric acid, patulin, moniliformin, and STC, were found to be the most common contaminants of grains and other feed products worldwide; the mean total concentration in this case of STC was 136μg/kg[4].

The recent study clarifies that the detection rate of contaminated feed samples was higher (26%) than for feed materials (6%). AFB_1 was detected at concentrations up to 0.1045mg/kg in cattle feed and 0.1234mg/kg in corn; ZEN was detected at concentrations up to 6.420mg/kg in sheep feed, while OTA was rarely recorded and at lower concentrations (up to 0.085mg/kg)[5].

The scientific novelty of the current work lies in the development of a highly flexible analytical system capable of determining these mycotoxins across various concentration ranges and *in silico* evaluation and presentation of their interactions.

1.1 Differences Between ChE

The main distinguishing feature of ChEs is their change in substrate specificity: acetylcholine is hydrolyzed by acetylcholinesterase (AchE) much faster than other choline esters, but this enzyme is less active against butyrylcholine. Conversely, both butyrylcholine and acetylcholine are very well hydrolyzed by Butyrylcholinesterase (BchE). Although its catalytic properties vary from species to species, it is generally more active on the synthetic substrates propionylcholine or butyrylcholine than on acetylcholine[6]. Butyrylthiocholine is not a physiological substrate in the human brain and is used as a substrate to differentiate the two types of ChEs[6]. Their tissue-specific distribution also differs from each other: AchE is known to be abundant in the brain, muscle, and red blood cell membrane, whereas BchE has a higher activity in the liver, intestine, heart, kidney, and lung[7]. It should be noted that the AchE and BchE enzymes are known markers for determining the degree of poisoning by certain neurotoxic compounds. The inhibition of these cholinesterase enzymes by various compounds is primarily used in *in vitro* studies. To clarify, inhibitors are a group of compounds used in pharmacology as drugs, in agriculture as pesticides, and in military applications as nerve agents. Some secondary metabolites have also been shown to inhibit ChEs.

Reversible inhibitors can spontaneously dissociate from ChEs. On the other hand, ChEs have limited applicability in the diagnosis of poisoning with reversible inhibitors[8]. It's important to note that biosensors can be considered a high replacement for traditional analytical methods due to their high selectivity and sensitivity. Heavy metals and pesticides are typically the most potent enzyme inhibitors, and it is precisely these types of biosensors, based on enzyme inhibition, that are widely used in environmental safety, food safety, and clinical analysis.

Selective mycotoxin detection requires the synthesis of specific antibodies. However, mycotoxins are non-immunogenic and therefore must be bound to suitable carrier proteins to elicit an immune response. Bovine serum albumin is typically used as the carrier protein[9]. Due to the high specificity of the antibody-antigen complex, it is possible to analyze both a single mycotoxin and a group of toxins from the same family. This method is very sensitive: for example, OTA was detected using Enzyme Linked Immunosorbent Assay (ELISA) with chemiluminescence detection, and the detection limit was 0.01μg/l. Despite the reliability of the ELISA method, it is more suitable for portable rather than laboratory analysis, as laboratory analysis is quite labor-intensive and requires specialized

readers. Furthermore, the disadvantages of using antibodies include their high immunogenicity, instability, and high cost[10].

A biosensor is an analytical device that includes three components: (1) a biological recognition element (e.g. enzymes, antibodies, nucleic acids, cells, etc.) that mediates a biochemical response; (2) a physicochemical transducer that converts the biological response into a measurable signal (e.g. current, heat, fluorescence); and (3) a detector that identifies the signal[1]. A biosensor is a device containing a closely related biologically derived molecule and a physicochemical transducer[11]. It has long been known that AchE and BchE are enzymes that are expressed in the human body under physiological conditions.

The AchE enzyme plays an important role in cholinergic nerves, where it hydrolyzes the neurotransmitter acetylcholine. Both enzymes are sensitive to inhibitors that act as toxic compounds, and, as noted, they can be inhibited by various compounds. Some of these are used as drugs to treat Alzheimer's disease, myasthenia gravis, or glaucoma. Mycotoxins such as ZEN, STC, OTA and DON also belong to the group of cholinesterase inhibitors.

In my co-authored work, the main problems and existing potential of biocatalytic transformation of various mycotoxins are highlighted[12]. ChEs can be used to create biosensors or other devices in which the enzyme is a recognition element[13].

1.1.2 Active Site of AchE and BchE

It's worth noting that three regions in the enzyme's structure play a key role in substrate conversion or interactions with various inhibitors: the active site, the aromatic cleft, and the peripheral (β) anion center. The latter two, the peripheral anion center and the aromatic cleft, represent a barrier to unwanted substrates, and each substrate must pass through them on its way to the enzyme's active site. The peripheral anion center is located on the enzyme's surface.

It is more developed in AchE than in BchE[14,15]. Amino acid residues Tyr 70, Asp 72, Tyr 121, Trp 279, and Tyr 334 (numbered for the Pacific electric eel) are responsible for cation-π and π-π interactions with substrates and inhibitors, resulting in conformational changes in the entire enzyme molecule[16]. The works[17,18] can serve as examples of binding of inhibitors to the peripheral anionic site of AchE. Another compound, huperzine A, can bind to both peripheral and α-anionic sites[19]. As the name suggests, the aromatic gorge of AchE is composed of aromatic amino acids and contains fourteen amino acid residues, while BchE has only eight[20]. The aromatic gorge acts as a selective network that selects which substrate enters the active site[21].

It's important to note that the active sites of the enzymes AchE and BchE are virtually identical. Three amino acid residues - Ser 200, Glu 327, and His 440 (numbered according to the Pacific electric eel) - are located in the ester region of the active site.

The esteric subsite is responsible for the hydrolysis of the ester bound in acetylcholine and other substrates[22]. Adjacent to the ester subsite in the active site is an α-anionic subsite. The α-anionic subsite is responsible for the correct orientation of the substrate to the esthetic subsite[23]. The routine assay for cholinesterase activity uses the Ellman method[24], which has been used for both ChEs. This method has proven sufficiently robust for use in routine biochemical assays. The Ellman method is inexpensive and provides fairly good results without the need for special sample handling or a specific apparatus. This method works with acetylthiocholine as a substrate for AchE or butyrylthiocholine as a substrate for BchE, however, other thioesters are also suitable for the reaction[25].

1.1.3 Reversibility of AchE and BchE Inhibition by Mycotoxins

Some aspects of the inhibition mechanism were important to establish the suitability or unsuitability of an enzyme for a screening assay. In the first case, whether the inhibition is reversible or irreversible is of decisive importance, since for irreversible inhibition it becomes important to use a low enzyme concentration to obtain a low detection limit, as in the case of pesticide detection[26,27].

On the other hand, in the case of reversible inhibition, there should be no change in the degree of inhibition when using different enzyme concentrations. This reversibility of the inhibition process allows for instantaneous mycotoxin analysis, which takes only 2 minutes. To develop the spectrophotometric assay, parameters such as pH, reaction time, temperature, and substrate concentration were evaluated. It has been confirmed that reversible inhibitors can bind to enzymes through weak non-covalent interactions, such as ionic, hydrophobic, and hydrogen bonds. Because reversible inhibitors do not form chemical bonds with the enzyme, they are quickly formed and easily disposed of. Similarly, the enzyme-inhibitor complex decomposes rapidly, unlike irreversible inhibition. Irreversible inhibitors covalently bind to the enzyme, causing chemical changes in the enzyme's active sites and cannot be reversed.

The primary role of irreversible inhibitors is to alter the shape of key amino acid residues required for enzymatic activity. They are known to contain reactive functional groups such as aldehydes, alkenes, or phenylsulfonates. Reversible inhibitors can spontaneously dissociate from ChEs. Dissociation occurs when blood or plasma samples are introduced into a cuvette and the sample is diluted with

other reagents during cholinesterase activity testing.

Notably, most irreversible inhibitors inhibit both AchE and BchE, while the amount of reversible AchE inhibitors does not affect BchE activity[28]. Selective BchE inhibitors such as tetraisopropylpyrophoramide are also known[29,30].

2 MATERIALS AND METHODS

Apparatus and Reagents. All chemicals from commercial sources were of analytical grade. AchE (EC 3.1.1.7) (PDB 1EEA (*Electrophorus Electricus*), BchE (*Bovine serum*) (EC 3.1.1.8) (PDB 1P0I (*Homo Sapiens*), S-acetylthiocholine iodide, S-butyrylthiocholine iodide, and 5,5-dithiobis-(2-nitrobenzoic acid (DTNB)) were obtained from Sigma Chemical Co. (St. Louis, MO). Mycotoxin stock solutions were prepared in methanol. Different concentrations of four mycotoxins were obtained by diluting the stock solution with methanol. Agilent 8453 UV/spectrophotometer was used for spectrophotometric measurements.

AchE activity was assessed by measuring the product of the enzymatic reaction. In the Ellman method, thiocholine, formed by the conversion of the enzyme from its thioester form, is reacted with 5,5-dithiobis-2-nitrobenzoic acid to form 5-thio-2-nitrobenzoic acid. Mycotoxins: ZEN (C18H22O5), STC (C18H12O6), DON (C15H20O6) and OTA (C20H18ClNO6). Specific enzyme substrates: athetylthiocholine (C7H16NOS+), butyrylthiochoiline (C9H20NOS+).

2.1 Work Methodology

Before proceeding with molecular docking[31], all structures of mycotoxins and specific enzyme substrates were optimized, minimized using Chem Bio 3D Ultra 12.0 software[32].

2.2 Procedure for Preparing Structures of Specific Substrates and Mycotoxins

All mycotoxin compounds and structures of specific substrates and co-crystal ligands were generated using ChemBioDraw (version 12.0, CambridgeSoft) and then energy minimization was sequentially applied to these compounds using the ChemBio3D software package using the MM2 force field.

The structures of the 1EEA and 1P0I enzymes in PDB format were converted to PDBQT format using AutoDockTools (as part of MGL Tools version 1.5.6., available at http://mgltools.scripps.edu/)[33-35] with atomic charges calculated by the built-in Gasteiger-Marsili. Two enzyme structures in PQR format were converted to PDBQT format using program AutoDockTools. Mycotoxins and specific substrate structures were attached to certain enzymes using the AutoDock Vina program (version 1.1.2. available at http://vina.scripps.edu/)[36,37]. The surface charge distribution of the 1EEA and 1P0I enzymes at their optimal pH 8 was calculated using the adaptive Poisson-Boltzmann solver (APBS. version 1.4.2.1) and the PDB2PQR servers (version 2.1.1) (available at http://www.poissonboltzmann.org/)[38,39] with force field PARSE and default settings. The grid, whose cell size was chosen based on the surface area of the enzyme molecule, was approximately centered on the active sites of each of the two enzymes used in this study. For the calculations, the program parameters were set to default values. It should also be noted that 10 model poses of mycotoxin structures were elected.

Affinities (kcal/mol) were obtained as the end result of molecular docking. All results of the analyses performed were interpreted and visualized using Molecular visualzation and graphics system (MVGS) PyMol (version 1.7.6. Schrödinger. LLC)[40,41].

Recently I wrote a manuscript reporting on the feasibility of enzymatic hydrolysis of three different mycotoxin molecules in the active sites of two different enzymes using molecular docking and comparing the results[42].

Overall, it can be said that in the field of drug development using computer systems, the molecular docking method plays an important and necessary role in the design and development of drug molecules, saving time, money, energy, and the environment.

With its origins firmly rooted in the developments in computational chemistry and structural biology, molecular docking has evolved from a theoretical concept into an intricate and vital tool in contemporary drug discovery[43-45]. Molecular docking studies showing strong binding affinities to significant proteins connected to inflammation and oxidative stress confirmed the observed biological activity[46]. The molecular docking simulation provided insights into bond interactions, revealing that hydrogen bond formation plays a crucial role in stabilizing the protein-ligand complexes[47,48].

2.3 Molecular Docking Procedure

The procedure for performing molecular docking and obtaining enzyme-specific substrate and enzyme-mycotoxin complexes is as follows: before starting molecular docking, it is necessary to load the PDB files of the 1EEA and 1P0I enzymes and the structures of all mycotoxins and specific substrates into the AutoDock Vina 1.1.2. Remove excess heteroatoms from the enzyme structure, after which it is necessary to set the grid parameters. For example, for the PDB 1P0I and enzyme, these parameters were as follows: center_x=137.901;center_y=122.764;center_z=38.655; size_x=30; size_y=34; size_z=38; for the PDB 1EEA enzyme these parameters were as follows: x=11.244; center_y=28.066; center_z=37.217 size_x=30; size_y=34; size_z=38.In each case, the exhaustiveness parameter was equal

https://doi.org/10.53964/jmab.2026001

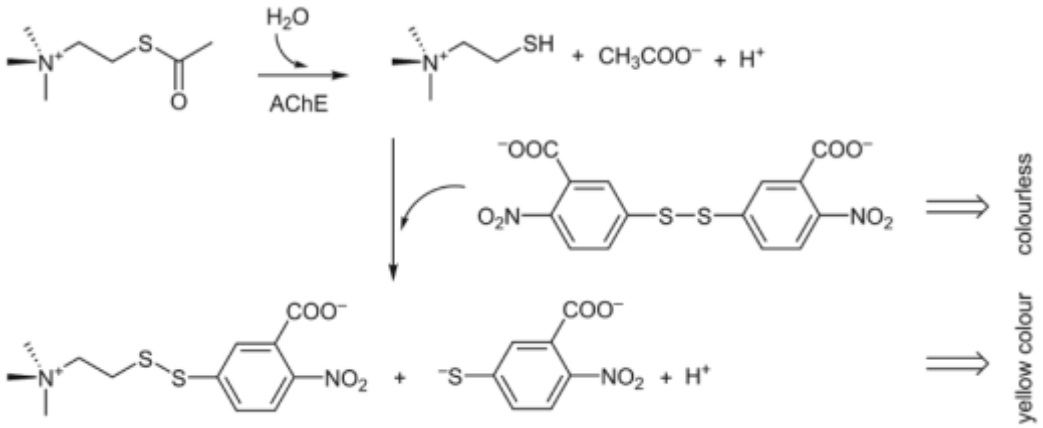
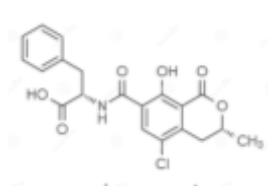
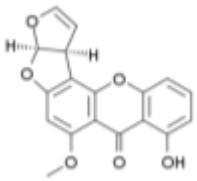
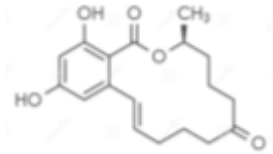
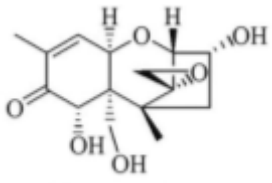
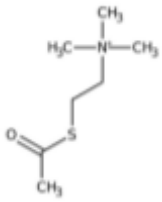
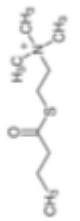
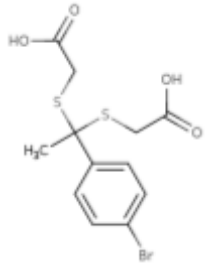
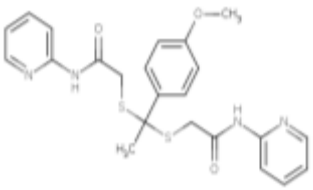
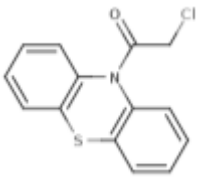
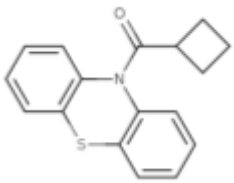
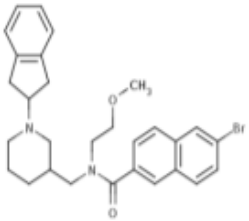
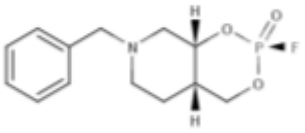


Figure 1. Reaction of the Ellman Spectrophotometric Method using the Example of AchE Enzyme.

Table 1. Molecular Structures of Chemical Compounds Used in this Study

OTA	STC	ZEN	DON
			
Acethylthiocholine	Butyrylthiocholine	2,2'-(1-(4-bromophenyl)ethane-1,1-diyl)bis(sulfanediyl)diacetic acid	2,2'-(1-(4-methoxyphenyl)ethane-1,1-diyl)bis(sulfanediyl)bis(N-(pyridin-2-yl)acetamide)
			
10-(Chloroacetyl)-10H-phenothiazine	10-(Cyclobutylcarbonyl)-10H-phenothiazine	(+)-(1R,3S,6S)-9-Benzyl-3-fluoro-2,4-dioxa-9-aza-3-phosphadecalin 3-oxide	(+/-)-6-Bromo-N-((1-(2,3-dihydro-1H-inden-2-yl)piperidin-3-yl) methyl)-N-(2-methoxyethyl)-2-naphthamide
			

to 8 and the number of binding modes was chosen as equal to 10. The substrate binding position and conformation were determined by molecular docking using the Autodock Vina 1.1.2 docking software.

A simplified diagram of cholinesterase-based biosensors is shown in Figure 1. Biosensors are suitable for the analysis of cholinesterase inhibitors, i.e., neurotoxic compounds that pose a serious risk to human health or life[14]. It's important to note that for the majority of ChE inhibitors, they act as biorecognition elements. This means that the presence of the analyte is manifested by an irreversible decrease in the signal provided by the enzyme activity. On the other hand, some reversible inhibitors are easily cleaved, restoring enzyme activity. The good commercial availability of ChE enzymes and reliable methods for assessing enzyme activity are the main advantages of this type of biosensor.

The Table 1 below includes the structures of all the main molecules used in the current study.

2.4 Preparation of Solutions

2.4.1 Preparation of 0.2M Phosphate Buffer

The phosphate buffer was prepared from two salts $K_2HPO_4 \cdot 3H_2O$ and KH_2PO_4. For 400ml of solution, a sample of $K_2HPO_4 \cdot 3H_2O$m=9.12g and KH_2PO_4m=5.44g were taken. The pH was tailored to 8 using 1M NaOH solution.

2.4.1.1 Preparation of 0.1M Phosphate Buffer

A 0.1M phosphate buffer of KH_2PO_4 salt m=5.44g was prepared in the same way.

2.4.1.2 Preparation of DTNB dye

To prepare a DTNB solution with a concentration of 20mmol/l, a sample of m=0.0119g was taken and dissolved in 1.5ml of phosphate buffer with pH=7, containing 1.5g/l Na_2CO_3.

2.4.1.3 Preparation of AchE Solution (0.01mg/ml)

A stock solution of the enzyme was prepared by dissolving 1mg of lyophilized enzyme in 1ml of distilled water. To prepare a 0.01mg/l AchE solution, 10µl were taken from the 1mg/ml stock solution and 990µl of phosphate buffered saline PBS (pH=7.4) were added. 0.05mg/l AchE was prepared in a similar way.

2.4.1.4 Preparation of BchE Solution (0.1mg/ml)

A 0.1mg/ml BchE solution was prepared in a similar way.

2.4.1.5 Preparation of Acetylthiocholine Iodide Substrate Solution

To prepare a 50mM substrate solution, a weighed portion of acetylthiocholine iodide m=0.0145g was taken and dissolved in 1 ml of distilled water. To prepare 25, 10, 2 mM substrate solutions, 50mM acetylthiocholine iodide solution was consecutively diluted with distilled water.

2.4.1.6 Preparation of Butyrylthiocholine Iodide Substrate Solution

Similarly, a 50mM butyrylcholine iodide substrate solution m=0.0159g was prepared. A 10mM substrate solution was netted by diluting a 50mM solution with distilled water.

2.4.2 Preparation of Mycotoxin Solutions

To prepare a stock solution of mycotoxins, 10mg ZEN, 1mg STC, 10mg OTA, 1mg DON were dissolved in 1 ml of methanol. Various other concentrations of mycotoxins used in the study were obtained by diluting the stock solution with methanol solvent.

2.4.2.1 Analysis Procedure

The rate of formation of thiocholine, a product of enzymatic hydrolysis of acetylthiocholine and butyrylthiocholine in the presence of AchE and BchE, respectively, was measured using the Ellman spectrophotometric method. The activity of AchE and BchE was estimated by measuring the rate of formation of the enzymatic reaction product and calculated using the Bouguer-Lambert-Beer law and the known molar extinction coefficient $\varepsilon=13.600M^{-1}cm^{-1}$, at a wavelength of 412nm. The spectrophotometric reaction was carried out in the presence of inhibitors - mycotoxins. Different amounts of the inhibitor were added to the reaction medium and calibration dependences of the residual activity on the inhibitor concentration were constructed based on the experimental results. Residual activity is the ratio of the enzymatic reaction rate in the subsistence of mycotoxin to the enzymatic reaction rate without inhibitor.

2.4.2.2 Determining the Standard Deviation of the Signal

For the purpose of establishing of the standard deviation of the signal, multiple measurements of the enzymatic reaction rate without inhibitor were performed. Several series of measurements of the enzymatic reaction rate without inhibitor were made, with two or three measurements in each series. The first measurement was taken as 100%, and consequentt values were expressed as a percentage in regard to the first. Origin 8 program was used to plot all the dependency graphs, and the standard deviation was found using the Sigma Plot 12.5 program for all measurements.

2.4.2.3 Enzymatic Hydrolysis of Acetylthiocholine Iodide by AchE

To determine the catalytic constants, a 50mM acetylthiocholine iodide solution was diluted sequentially 1-20 times and a reaction was carried out with each substrate concentration: 1950µl of 0.2M phosphate buffer (pH 8), 20µl of DTNB solution, 10µl of 0.05mg/ml AchE and 20µl of 50mM substrate were placed in a 2ml spectrophotometric cuvette. The measurement was carried out for 1 minute. The data were nearly accurate by a hyperbolic dependence in the OriginPro 8.1 program.

2.4.2.4 Enzymatic Hydrolysis of Acetylthiocholine Iodide by AchE in the Existence of Mycotoxins

In order to determine the type of inhibition in the presence of ZEN, 1940µl of 0.2M phosphate buffer, 20µl of DTNB, 10µl of 0.05mg/ml AchE, 10µl of 10mg/ml ZEN and 20µl of 50mM acetylthiocholine iodide were fixed in a 2ml spectrophotometric cuvette. The reaction was carried out correspondingly at initial inhibitor concentrations of 1 and 0.5mg/l and at initial substrate concentrations of 25 and 10mM. For the control measurement, 20µl of methanol were added instead of the inhibitor. The measurement was carried out for 1min. To construct a calibration dependence of the residual enzyme activity on the inhibitor concentration, the mycotoxin was diluted sequentially from an initial concentration of 10mg/ml ZEN with 1mg/ml STC, 10mg/

ml OTA and 1mg/ml DON by 1-20 times. 1840µl of 0.1M phosphate buffer, 20µl of DTNB, 20µl of 0.01mg/ml AchE, 20µl of mycotoxin and 100µl of 2mM acetylcholine iodide were placed in a 2ml spectrophotometric cuvette. For the control measurement, 20µl of methanol were added instead of the inhibitor. In the case of the DON mycotoxin, 100µl and 1760µl of buffer were added to the spectrophotometric cuvette. The measurements were carried out for 2min.

2.4.3 Enzymatic Hydrolysis of Butyrylthiocholine Iodide by BchE

To determine the catalytic constants, 10mM butyrylthiocholine iodide solution was diluted 1-20 times and a reaction was carried out with each concentration: 1820µl of 0.1M phosphate buffer, 20µl of DTNB, 20µl of 0.1mg/ml BchE, 20µl of ZEN and 100µl of butyrylthiocholine iodide were placed in a 2ml spectrophotometric cuvette. The measurements were carried out for 2min. The data were approximated by a hyperbolic dependence in the OriginPro 8.1 program.

2.4.3.1 Enzymatic Hydrolysis of Butyrylthiocholine Iodide by BchE in the Presence of Mycotoxins

To construct a calibration dependence of the residual enzyme activity on the inhibitor concentration, the mycotoxin was thinned consecutively from an initial concentration of 10mg/ml ZEN with 1 mg/ml STC, 10mg/ml OTA and 1mg/ml DON by 1-20 times. A reaction was carried out with each concentration: 1820µl of 0.1M phosphate buffer, 20µl of DTNB, 40µl of 0.2mg/ml BchE, 20µl of ZEN and 100µl of 5mM butyrylthiocholine iodide were placed in a 2ml spectrophotometric cuvette. In the case of the mycotoxin DON, 100µl of buffer was added to the spectrophotometric cuvette, 1740µl. The dimension was carried out for 2min.

2.4.3.2 AchE Activity Measurement Reaction Method

AchE activity was determined using Ellman's method. Briefly, 100µl of 2mM acetylthiocholine iodide (Sigma, USA) and 20µl of 20mM 5,5'-dithiobis (2-nitrobenzoic acid) (Sigma, USA) in 0.1M phosphate buffer (pH 7.0) containing 1.5g/l Na_2CO_3 were added to 1.84ml of 0.1M phosphate buffer (pH 8.0) in a spectrophotometric cell. After that, 20µl (40µl in the case of BchE) of AchE were added and the formation rate of 2-nitro-5-thiobenzoic acid was determined at λ=412nm. One unit of AchE or BchE activity was determined as the quantity of enzyme that hydrolyzed 1 µmol of substrate per minute at 25 °C.

2.4.3.3 Reaction Procedure for Measuring BchE Activity

Briefly, 100µl of 5mM acetylthiocholine iodide (Sigma, USA) and 20µl of 20mM 5,5'-dithiobis (2-nitrobenzoic acid) (Sigma, USA) in 0.1M phosphate buffer (pH 7.0) containing 1.5g/l Na_2CO_3 were added to 1.82ml of 0.1M phosphate buffer (pH 8.0) in a spectrophotometric cell. Afterwards, 40µl of BchE were added and the rate of formation of 2-nitro-5-thiobenzoic acid was determined at λ=412nm.

2.4.3.4 Gauging the Effect of Methanol on AchE and BchE Inhibitions

The aftermath of methanol on AchE and BchE inhibition was also assessed. A 1.84µl aliquot of phosphate buffer solution (0.1M, pH8.0) including a known amount of AchE and methanol (20µl) was added in the absence or presence of various mycotoxin concentrations.

The substrate was then added, and residual enzyme activity was assessed using the procedure described above. Residual enzyme activity (I%) was calculated using formula 1, where A_0 is the optical density obtained in an aqueous solution containing methanol, and A_i is the optical density obtained in an aqueous solution containing methanol as the solvent and the mycotoxin:

$$I\% = A_i/A_0 * 100 (1)$$

3 RESULTS

Since the goal of the current study firstly included developing an *in vitro* assay that can measure the lowest possible concentrations of mycotoxins, it studied the inhibition possibility of mycotoxins using AchE, and BchE enzymes. This was also demonstrated using the molecular docking method applied, which will be discussed in detail later.

Figures 2 and 3 show the resulting graphical dependences of the residual activities of both enzymes after the inhibitory effects of four mycotoxin molecules on them.

For quantitative data analysis, graphs of residual activity (%) of both ChEs versus CH_3OH concentration as a solvent are plotted.

As Figure 4 shows, in the control experiment, as the CH_3OH concentration in the medium increased, the residual activity of both enzymes gradually decreased.

As also shown in Figure 4, solvent CH_3OH tested decreased AchE, BchE activities having the smallest effect. Overall, while the effect of the solvent on BchE activity was less than AchE, solvent CH_3OH tested affected both enzymes activity slightly negligible.

In general, evaluating a range of structurally similar compounds, such as a series of alcohols, can help better determine the contribution of polarity to the inhibition of a particular enzyme. If the cosolvent acts as a competitive inhibitor with the substrate, as in this case, then in the simplest case the cosolvent is expected to increase the K_m value for the substrate without affecting V_{max}.

Scholars conducted a similar study for human

https://doi.org/10.53964/jmab.2026001

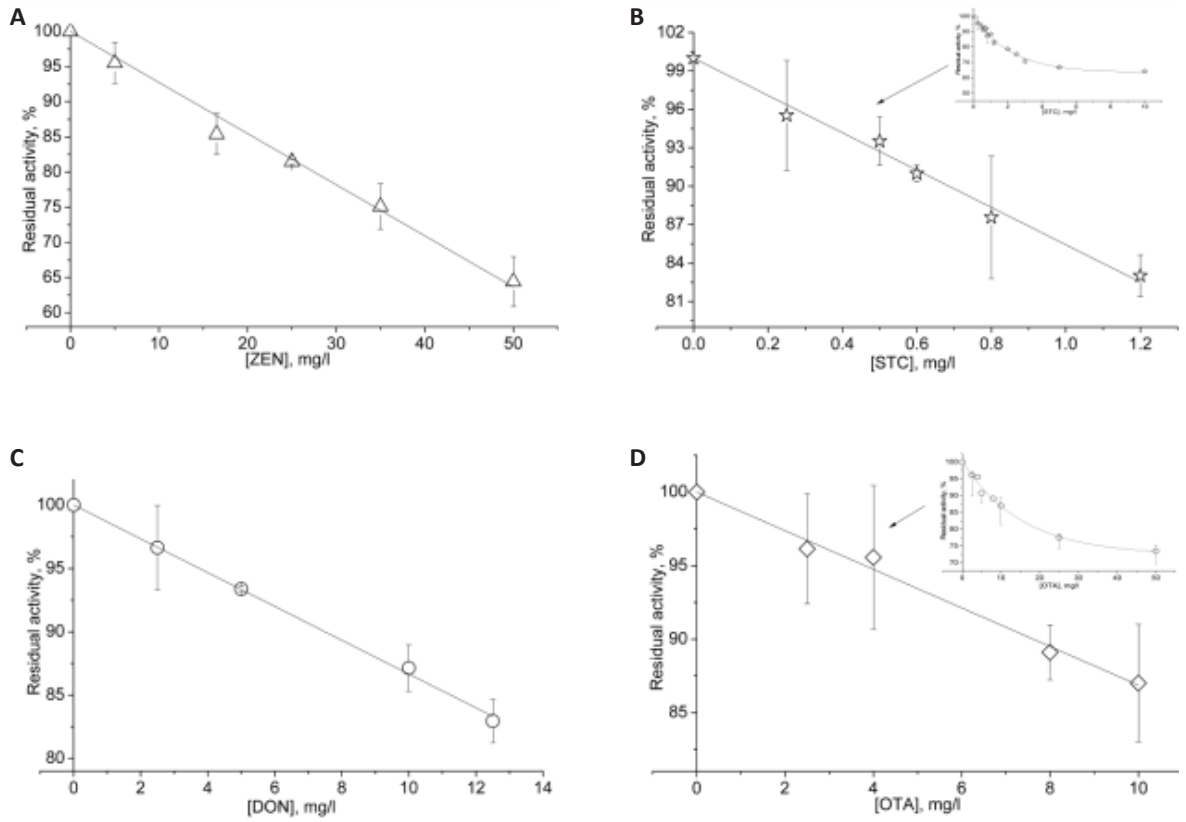


Figure 2. Inhibition Effects of Mycotoxins ZEN (A), STC (B), DON (C) and OTA (D) on AchE Enzyme Activity.

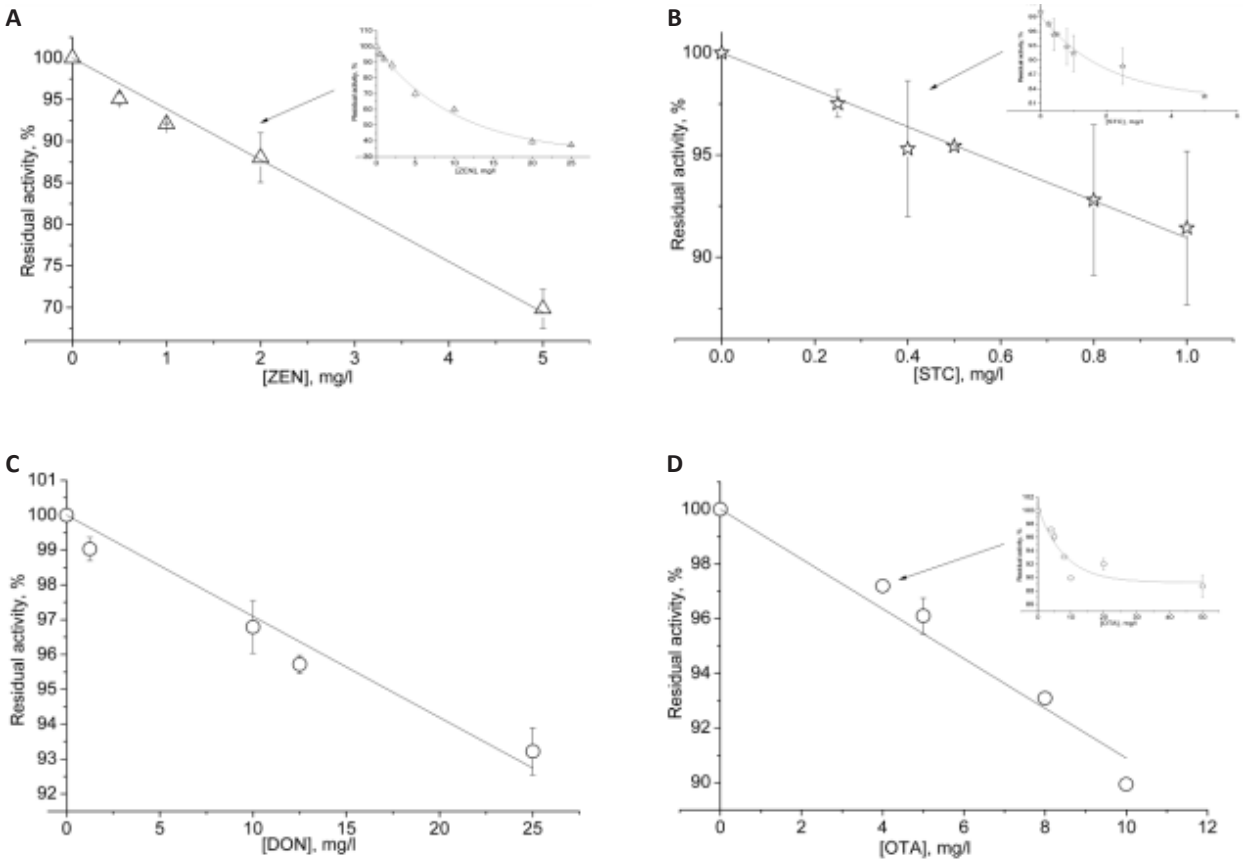


Figure 3. Inhibition Effects of Mycotoxins ZEN (A), STC (B), DON (C) and OTA (D) on BchE Enzyme Activity.

https://doi.org/10.53964/jmab.2026001

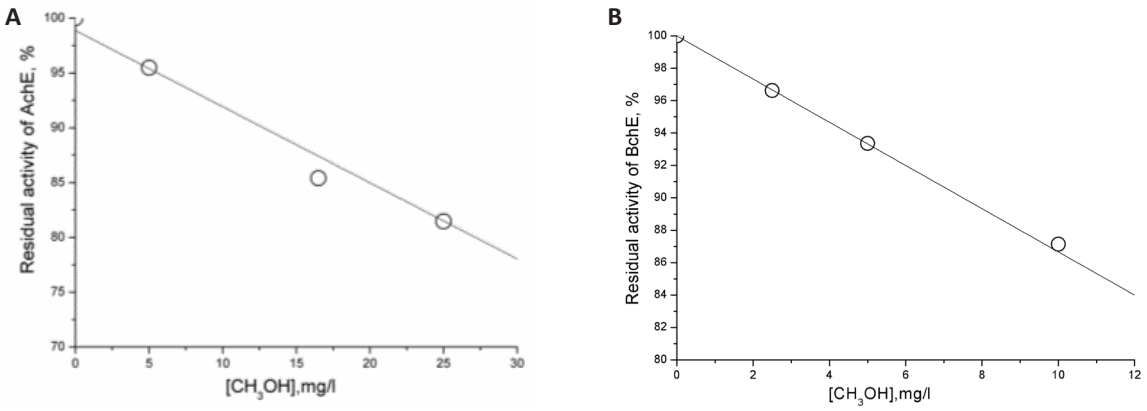


Figure 4. Plot of Residual Activities (%) of ChEs (A,B) in the Presence of a Control Solvent CH_3OH.

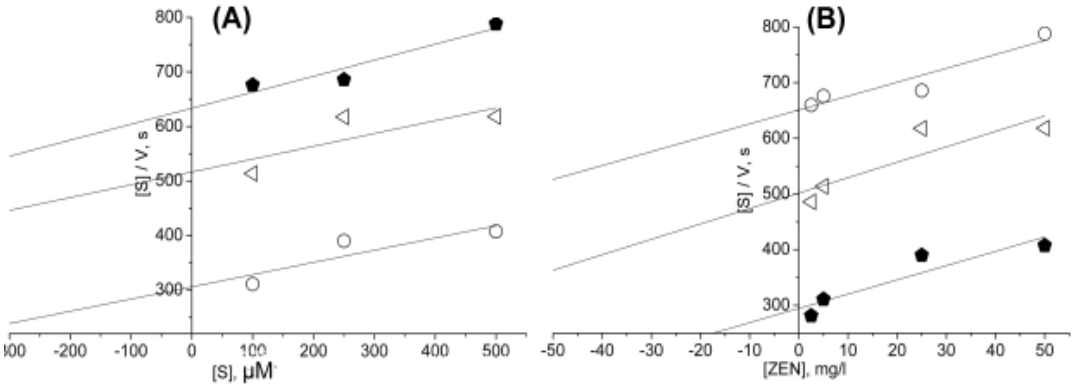


Figure 5. Determination of the Inhibitory Constant by the Dixon Method (A) and the Cornish-Bowden Method (B) at an Ionic Strength of the Buffer Solution I=0.2M at Different Substrate Concentrations: 0.5mM (⬟); 0.25mM (◁); 0.1mM (○).

recombinant AchE and reported estimated K_i values of 4200, 360, 177, and 81mM for methanol, acetonitrile, acetone, and DMSO. It is stated that comparison to BchE shows that the BchE K_i values are approximately 10-fold higher for acetonitrile and acetone and approximately 20-fold higher for DMSO as the cosolvent[49].

As also noted[50] in a recent study, methanol demonstrated little effect on enzyme inhibition and kinetics, demonstrating its suitability for AchE analysis.

For a competitive inhibitor (Figure 5B) the lines converge above the x-axis and the [I] value where they intersect is $-K_i$. A competitive inhibitor is a compound that has a structural similarity with the substrate. With this type of inhibition, K_m increases. The reaction rate is reduced because the enzyme-inhibitor complex is inactive (does not break down to form products).

The Michaelis constant of AchE with acetithiocholine iodide as a substrate is 98.12μM (Figure 6A). From Figures 5 and 6B it can be concluded that at a given ionic strength of the solution, a competitive type of inhibition of the AchE enzyme is observed. The inhibitor constant K_i is an indicator of how strong the inhibitor is; it is the concentration required to obtain half the maximum inhibition. In virtually every case, competitive inhibitors bind in the same binding site as the substrate, but same-site binding is not a requirement. A competitive inhibitor could bind to an allosteric site of the free enzyme and prevent substrate binding, as long as it does not bind to the allosteric site when the substrate is bound.

A 2-fold decrease in the ionic strength of the buffer solution leads, as can be seen, to an increase in the Michaelis constant. Figure 7 shows a graphical determination of the Michaelis constant by the hyperbolic method for the enzyme BchE with butyrylthiocholine iodide as the substrate S at an ionic strength of the buffer solution equal to 0.1M.

From Figure 7 it follows that the Michaelis constant is 319.33μM.

3.1 Determination of the Type and Constant of Inhibition using the Example of Mycotoxin - ZEN and Enzyme AchE

To determine the type of inhibition at each inhibitor concentration of 50, 5, 2.5mg/l in the cuvette, the following dependencies were constructed: S/V versus S and V versus V/S, where S acts as the substrate concentration and V is the rate of the enzymatic reaction in the presence of the inhibitor. Based on the location of the graphs, it can be concluded that ZEN is a competitive inhibitor (see Figure 8)[51].

https://doi.org/10.53964/jmab.2026001

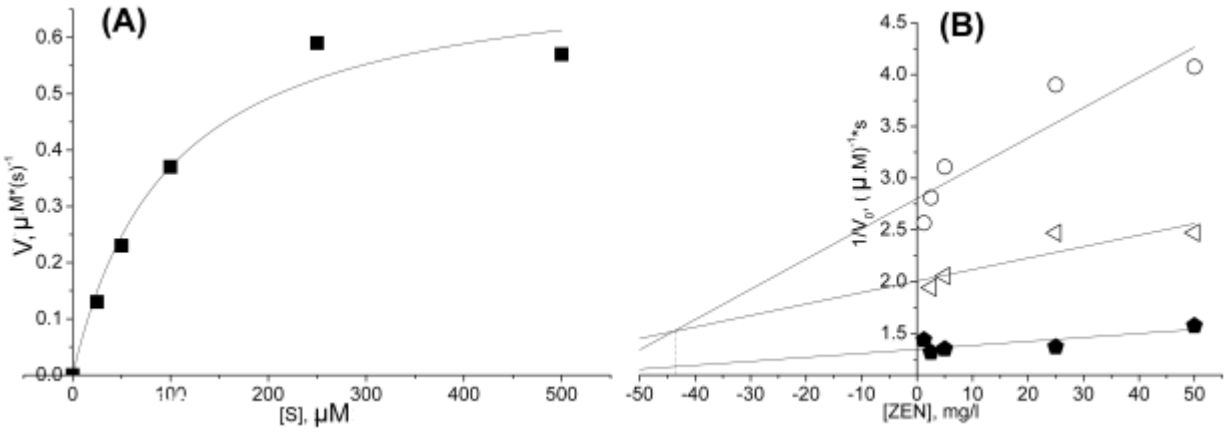


Figure 6. Determination of the Michaelis Constant K_m (μM) for the AchE Enzyme using the Hyperbolic Method (A) and the Inhibitory Constant using the Dixon Method (B) at an Ionic Strength of the Buffer Solution I=0.2M at Different Substrate Concentrations: 0.5mM (⬟); 0.25mM (◁); 0.1mM (○).

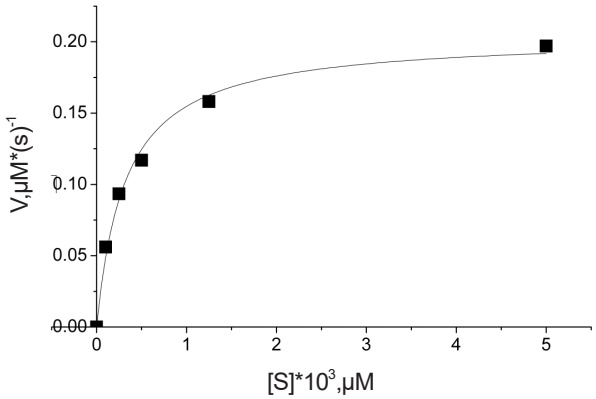


Figure 7. Determination of the Michaelis Constant by the Hyperbolic Method for the BchE Enzyme with Butyrylthiocholine Iodide as the Substrate S at the ionic Strength of the Buffer Solution Equal to 0.1M.

In order to determine the inhibition constant at each concentration of ZEN 50, 5, 2.5mg/l in the cuvette, graphs of the dependence of the enzymatic reaction rate on the substrate concentration were plotted and the corresponding apparent Michaelis constants were found, K_m' - 408±124, 212±66 and 258±117μmol/l, respectively. The inhibition constant was estimated by plotting the dependence of the obtained K_m' values on the concentration of inhibitor I was calculated using the formula $K_m+(k_m*I)/k_i$ K_m'=97, 8+6, 52*I $K_i=K_m/6{,}52=15{,}0$μmol/l. Taking into account the standard deviation K_i=15±4μmol/l*s. Figure 9 shows the graphical dependence of the apparent Michaelis constant on the inhibitor mycotoxin ZEN concentration.

To describe a more rigorous kinetic analysis for determining the inhibition constant for the mycotoxin inhibitor ZEN, in a software Origin 8.1 a nonlinear regression (NLR) plot (see Figure 10) was used to plot dependence between the apparent Michaelis constant versus the mycotoxin inhibitor ZEN concentration.

The graph of this nonlinear regression relationship is described by the following equation: $y=V_{max}\,x_n/(k_n+x_n)$

According to Figure 10, the inhibition constant K_i value obtained is identical to the previous calculation method.

4 DISCUSSION

In the case of the AchE enzyme, which was initially taken in a 100-fold short dilution (the initial concentration of which was C_0=1mg/ml), it should be noted that the addition of 5mg/ml ZEN to the spectrophotometric cuvette already leads to inhibition of the AchE enzyme by 5%, whereas for the BchE enzyme, the same concentration of mycotoxin, which is the maximum of the detectable range, leads to a decrease in the residual activity of this enzyme by 30.14%.

This means that the sensitivity in the case of BchE will be higher in relation to ZEN, since the range of detectable concentrations is narrow compared to AchE. The BchE enzyme is inhibited by 5% with just 0.5mg/L of the mycotoxin ZEN added to the spectrophotometric cuvette. For STC, which is the most sensitive to both enzymes (see Table 2), its amount inhibits the AchE enzyme by 6.5%, while the same amount of mycotoxin STC leads to a 4.6% reduction in residual BchE activity.

Although the operating range of concentrations is narrow in the case of the BchE enzyme, the detection limit (mg/l) is equal for AchE with mycotoxin STC (see Table 2). At a mycotoxin concentration of 0.25mg/l, the residual activity decreases by 4.5% and 2.5% for both AchE and BchE, respectively, indicating that AchE is the most sensitive enzyme. It is known that the solubility of mycotoxin DON in 100% ethanol is 10mg/ml.

In order to inhibit ChE, it was necessary to increase the volume of the mycotoxin DON inhibitor introduced by 5 times, in other words, to add 100 μl of the inhibitor to the cuvette. Mycotoxin DON was diluted 20-fold in the reaction with both the first and second enzymes, in contrast to the other three mycotoxins, for each of which a 100-fold

https://doi.org/10.53964/jmab.2026001

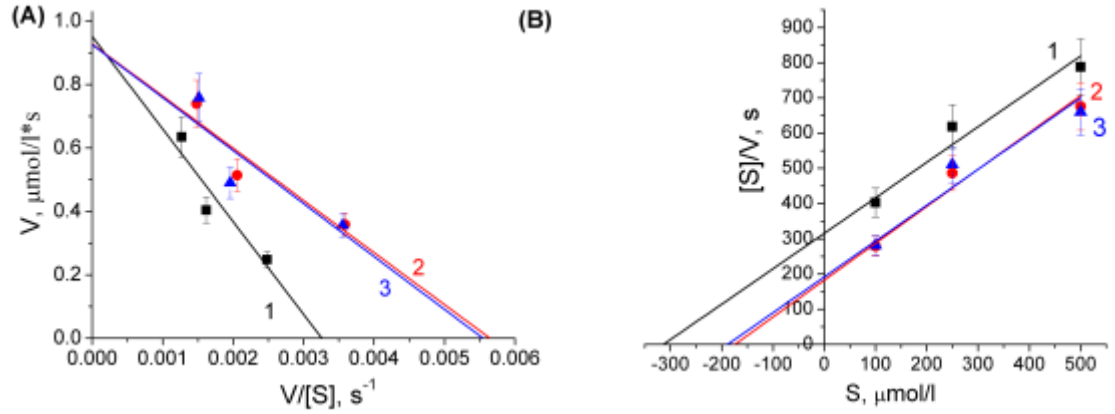


Figure 8. Graphic Dependences of S/V on S (A) and V on V/S (B) in the Appearance of the Inhibitor – ZEN; 1-50mg/l, 2-5mg/l, 3-2.5mg/l – Concentrations of Mycotoxin ZEN.

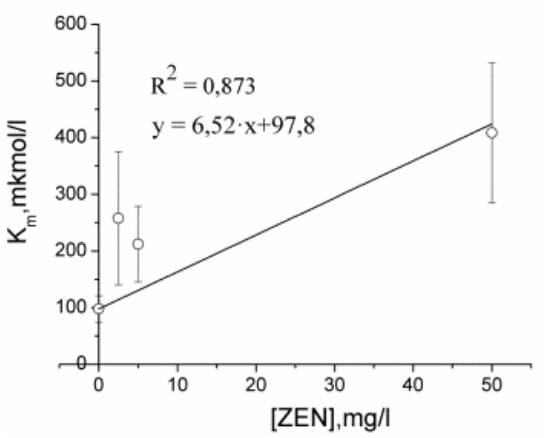


Figure 9. Graphical Dependence of значений от Values on the Concentration of Inhibitor Mycotoxin ZEN.

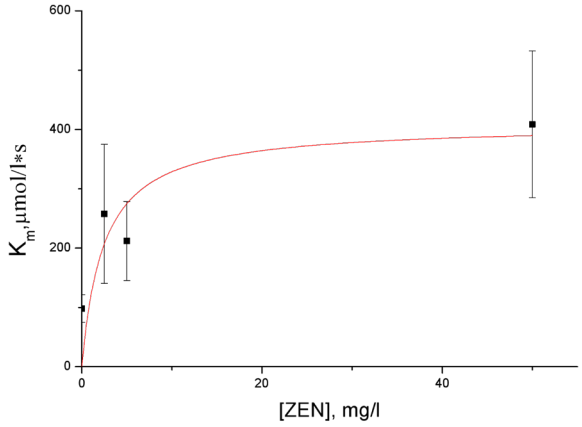


Figure 10. Graphical Dependence of the Apparent Michaelis Constant on the Concentration of the Mycotoxin Inhibitor ZEN using the Nonlinear Regression Function in the Growth/Sigmoid Category and the Hill Function.

Table 2. Detection Limits (mg/l) for Four Different Mycotoxins Obtained from the Spectrophotometric Ellman Reaction with the Enzymes AchE and BchE.

Mycotoxin	Enzyme AchE			Enzyme BchE		
	Equation of a straight line, R^2	LOD,mg/l	Operating range, mg/l	Equation of a straight line,R^2	LOD,mg/l	Operating range, mg/l
ZEN	y=100-0.727*x, R^2=0.999	5	5-50	y=100-6.116*x, R^2=0,999	0.5	0.5-5
STC	y=100-14,556*x, R^2=0.999	0.25	0.25-1.2	y=100-9,052*x, R^2=0,999	0.25	0.25-0.8
DON	y=100-1.333*x, R^2=0.999	2.5	2.5-12.5	y=100-0.29*x, R^2=0.999	1.25	1.25-25
OTA	y=100-1.312*x, R^2=0,.99	2.5	2.5-10	y=100-0.91*x, R^2=0.999	4	4-8

dilution of the inhibitor was observed. If we compare the sensitivities of these two ChEs with respect to mycotoxin DON, we will see that adding the same amount of inhibitor (10mg/l) leads to inhibition by 12.9% in the case of AchE and 3.2% in the case of BchE enzyme.

As for the OTA mycotoxin inhibitor, for example, if we take the mycotoxin concentration equal to 8 mg/l, then inhibition of 10.9% and 6.9% is observed for AchE and BchE, respectively. The AchE enzyme is most sensitive to OTA compared to BchE (see Table 2).

According to decreasing sensitivity to the AchE enzyme, these four mycotoxins can be arranged in the following row: STC>OTA>DON>ZEN.

By analogy, as in the case of the first enzyme, for BchE enzyme, according to the sensitivity parameter of the inhibitor-mycotoxin method, we can arrange them in the following row: STC>ZEN>DON>OTA.

Table 3. Characteristics of Enzymatic Catalysis for AchE and BchE Enzymes.

Enzyme	K_m (μmol/l)	$\frac{V_{max}}{E_0}$ (min^{-1})	$\frac{V_{max}}{E_0 \cdot K_m}$ (l/μmol*min)
AchE	98±23	316±26	3.22±1.02
BchE	319±35	8.3±0,2	0.027±0.003

The substrate concentration should be less than or equal to the Michaelis constant so that the reaction could be carried out in the kinetic mode, that is, in the linear range of the enzymatic reaction rate dependence on the substrate concentration. The detection limit was calculated using the formula $c\frac{3s_0}{S}_{min}$, where c_{min} is the detection limit, s_0 is the standard deviation of the signal, S is the sensitivity coefficient and is found from the equation $y=Sc+y_0$. Using the obtained rate data, the standard deviation of the background signal was calculated for AchE and BchE enzymes. The standard deviation of the background signal was 1.68% for AchE, and 1.58% for BchE. To determine the operating range, it is necessary to find the lower limit of the detectable content, which characterizes the minimum component content that can be determined with a given degree of accuracy. To estimate the detection limit, the formula used: $C_н=3.3 \bullet C_{min}$. For validating analytical performance, the signal-to-noise ratio was determined and it was obtained 3:1.

In a study[52] conducted a couple of years ago, a known amount of pure active ingredients is added to a blank sample - a sample containing all other ingredients except the active ingredient, the resulting mixture is analyzed, and the results are compared with predicted ones.

The limit of detection (LOD) is determined by analyzing samples with known analyte concentrations and establishing the minimum level at which the analyte can be detected. This method can be used for both instrumental and non-instrumental methods. This signal-to-noise ratio approach is only applicable to analytical methods with baseline noise. It is performed by comparing the measured signals from samples with known low analyte concentrations with the signals of blank samples and establishing the minimum concentration at which the analyte can be detected. A signal-to-noise ratio of 2:1 or 3:1 is commonly accepted. Response standard deviation and slope: $LOD=\frac{3.3\sigma}{S}$, where σ=response standard deviation. S=slope of the analyte calibration curve relative to the regression line.

Furthermore, it is known that the noise level does not change over time due to the detection mode[53].

A recently published study found that low resolution can lead to a low signal-to-noise ratio, which is critical for detecting trace amounts of analytes. This process played a key role in reducing background noise, improving enzyme-substrate binding, and increasing overall detection efficiency. Each of these parameters was optimized to increase the sensitivity and selectivity of the aptasensor for detecting some mycotoxins, ensuring a low LOD, and reducing background noise in complex matrices[54].

Based on the obtained equations (Figures 6 and 7), the values of K_m and V_{max}/E_0 and $V_{max}/(E_0 \bullet K_m)$ were calculated (see Table 3).

Founded on the results in the Table 3, it can be completed that the efficiency of catalysis of acetylthiocholine iodide hydrolysis by AchE is higher than the efficiency of catalysis of butyrylcholine iodide hydrolysis by BchE, because the $V_{max}/(E_0 \bullet K_m)$ value for AchE is greater than for BchE. The obtained K_m were used to estimate the amount of substrate that must be added to the reaction medium to carry out the enzymatic reaction in the presence of mycotoxin.

The obtained K_m were used to estimate the amount of substrate that must be added to the reaction medium to carry out the enzymatic reaction in the presence of mycotoxin. The amount of substrate should be such that the rate of the enzymatic reaction is in the linear range. Therefore, for the enzymatic reaction in the presence of AchE, the concentration of acetylthiocholine iodide in the cuvette is 98μM, and for BchE – 319μM butyrylthiocholine iodide in the cuvette.

The volume of the cuvette is 2000μl, and the volume of the added substrate (V_0) is 100μl. Then the initial concentration of acetylthiocholine iodide and butyrylthiocholine iodide in Eppendorf (C_0) is calculated using the formula:

$C_0=(V_{cuvette}*C_{incuvette})/(V_0*1000)=(2000*97,8)/(100*1000)=1.96$мМ–acetylthiocholine iodide

$C_0=(V_{cuvette}*C_{incuvette})/(V_0*1000)=(2000*312)/(100*1000)=6.24$мМ–butyrylthiocholine iodide

For convenience, it was decided to take 2mM acetylthiocholine iodide and 5mM butyrylthiocholine iodide, since the rate at these concentrations also lies in the linear range.

4.1 Molecular Docking Approach for Predicting the Binding of the Studied Specific Substrates and Mycotoxins in Active Centers of AchE and BchE Enzymes

The competitive type of inhibition was also confirmed using the molecular docking approach to prove the incorporation of mycotoxins into the active sites of the corresponding ChEs.

Figure 11 shows the position of the mycotoxin OTA near the catalytic triad of the enzymes AchE using MVGS PyMol.

It is interesting to note that as a result of searching and

https://doi.org/10.53964/jmab.2026001

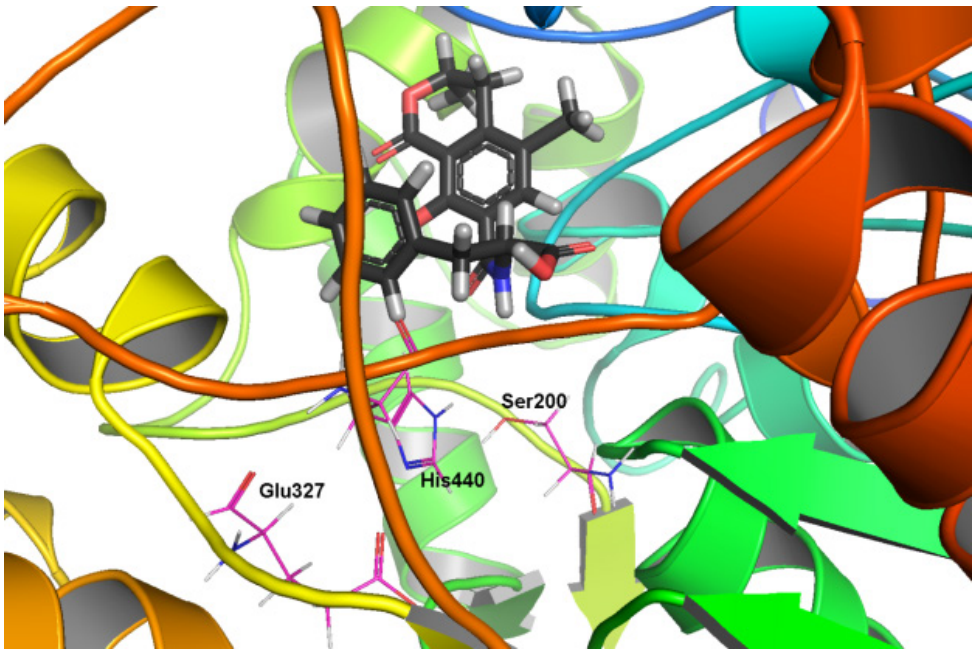


Figure 11. Representation of the Mycotoxin OTA Next to the Catalytic Triad of the Enzyme AchE using MVGS PyMol.

Table 4. STEADY State Turnover of Butyrylthiocholine by Bovine BchE and Inhibition of Butyrylthiocholine Turnover by using the Inhibitor as an Example Ethopropazine

	K_m, µM	Kss, mM	k_{cat}, min^{-1}	b	bk_{cat}, min^{-1}	K_i ethopropazine, µM	Reference
Bovine BchE	35	500	54,100	1.9	103,000	2.2	[55-57]
Human BchE	20–28	1.5	25,000–27,000	3.1–3.4	80,000–90,000	0.16; 0.2	[20,56,61]

comparing amino acid sequences, a 91% similarity was found between the enzyme from *Homo Sapiens* PDB 1P0I and the amino acid sequence isolated from the *Bovine Serum* organism. To expand the translational significance of the results obtained, the text below demonstrates how structural differences between BchE enzymes (Human and Bovine) may influence inhibitor binding and catalytic efficiency

The result of the alignment of the amino acid sequence of two enzymes: BchE *(Human)* and BchE (*Bovine serum*) is shown below on the Figure 12.

The amino acid sequence of Bovine BchE (accession number P32749) is 91% identical to that of Human BchE (accession number P06276). Both have a 28-amino acid signal peptide followed by 557 amino acids for the mature protein.

The quaternary structure of Bovine BchE is likely to be highly similar to that of Human BchE. The Human BchE structure can be found in Protein Data Bank record 1P0I[39]. Bovine BchE has the consensus sequence for 8 Asn-linked glycans, whereas Human BchE has been demonstrated to have 9 Asn-linked glycans.

Residues that form salt bridges in Human BchE are at the same positions in Bovine BchE (Arg42-Glu90, Arg147-Asp170, Arg265-Glu161, Arg515-Asp395). Forty residues at the *C*-terminus that constitute the tetramerization domain are essentially identical for the two enzymes, except for a Trp to Arg substitution at position 541, where Human BchE has tryptophan and Bovine BchE has arginine. Both BchE proteins have the catalytic triad residues Ser198, Glu325, His438, the choline binding site Trp82, the peripheral site residues Asp70, Tyr332, and the acyl binding pocket Leu286, Val288, Trp231. Bovine plasma esterase does not hydrolyze benzoylcholine, though benzoylcholine is a good substrate for Human BchE. Bovine plasma esterase hydrolyzes acetylcholine iodide at a rate of 76 nmoles per ml per min at pH 7.4, 30°C and acetylthiocholine iodide at a rate of 149 nmoles per ml per min at pH 8, 25°C. Based on these observations, it is generally accepted that bovine plasma contains AchE, but not BchE[55,56]. To answer the question of how structural differences might affect inhibitor binding or the catalytic efficiency of both enzymes, see Table 4 below, which includes confirmed information as an example of the inhibitor ethopropazine discussed by the authors in the literature.

Table 4 shows that the BchE-specific inhibitor ethopropazine inhibited Bovine BchE with a Ki of 2.2µM, which is 10-fold weaker than for Human BchE. The Ki value was measured using 0.05-2mM butyrylthiocholine and 0-15µM ethopropazine[56].

Catalytic efficiency is defined as a measure derived from the turnover number k_{cat} and the K_m values, which reflects

https://doi.org/10.53964/jmab.2026001

```
(Human)Query   1    EDDIIIATKNGKVRGMQLTVFGGTVTAFLGIPYAQPPLGRLRFKKPQSLTKWSDIWNATK  60
                    E+DIII TKNGKVRGM L V GGTVTAFLGIPYAQPPLGRLRFKKPQSLTKW DIWNATK
(Bovine)Sbjct  29   EEDIIITTKNGKVRGMHLPVLGGTVTAFLGIPYAQPPLGRLRFKKPQSLTKWPDIWNATK  88

(Human)Query   61   YANSCCQNIDQSFPGFHGSEMWNPNTDLSEDCLYLNVWIPAPKPKNATVLIWIYGGGFQT  120
                    YANSC QN DQSFPGF GSEMWNPNTDLSEDCLYLNVWIP PKPKNATV+IWIYGG FQT
(Bovine)Sbjct  89   YANSCYQNTDQSFPGFLGSEMWNPNTDLSEDCLYLNVWIPTPKPKNATVMIWIYGGSFQT  148

(Human)Query   121  GTSSLHVYDGKFLARVERVIVVSMNYRVGALGFLALPGNPEAPGNMGLFDQQLALQWVQK  180
                    GTSSLHVYDGKFLARVERVIVVSMNYRVGALGFLALPGNPEAPGN+GLFDQQLALQWVQK
(Bovine)Sbjct  149  GTSSLHVYDGKFLARVERVIVVSMNYRVGALGFLALPGNPEAPGNVGLFDQQLALQWVQK  208

(Human)Query   181  NIAAFGGNPKSVTLFGESAGAASVSLHLLSPGSHSLFTRAILQSGSFNAPWAVTSLYEAR  240
                    NIAAFGGNPKSVTLFGESAGAASVSLHLLSP SH LFTRAILQSGS NAPWAVTS YEAR
(Bovine)Sbjct  209  NIAAFGGNPKSVTLFGESAGAASVSLHLLSPESHPLFTRAILQSGSSNAPWAVTSRYEAR  268

(Human) Query  241  NRTLNLAKLTGCSRENETEIIKCLRNKDPQEILLNEAFVVPYGTPLSVNFGPTVDGDFLT  300
                    NRTL LAK  GCSREN+TEIIKCLRNKDPQEIL +E FVVPYGT LSVNFGPTVDGDFLT
(Bovine)Sbjct  269  NRTLTLAKFIGCSRENDTEIIKCLRNKDPQEILRHEVFVVPYGTLLSVNFGPTVDGDFLT  328

(Human) Query  301  DMPDILLELGQFKKTQILVGVNKDEGTAFLVYGAPGFSKDNNSIITRKEFQEGLKIFFPG  360
                    DMPD LL+LGQFKKTQILVGVNKDEGTAFLVYGAPGFSKDNNSIITRKEFQEGLKIFFPG
(Bovine)Sbjct  329  DMPDTLLQLGQFKKTQILVGVNKDEGTAFLVYGAPGFSKDNNSIITRKEFQEGLKIFFPG  388

(Human) Query  361  VSEFGKESILFHYTDWVDDQRPENYREALGDVVGDYNFICPALEFTKKFSEWGNNAFFYY  420
                    VSEFGKESILFHY DW+DDQR E YREAL DVVGDYN ICPALEFTKKFS+ GNNAFFYY
(Bovine)Sbjct  389  VSEFGKESILFHYMDWLDDQRAEKYREALDDVVGDYNIICPALEFTKKFSDMGNNAFFYY  448

(Human) Query  421  FEHRSSKLPWPEWMGVMHGYEIEFVFGLPLERRDQYTKAEEILSRSIVKRWANFAKYGNP  480
                    FEHRSSKLPWPEWMGVMHGYEIEFVFGLPLERR  YTKAEEI SRSI+KRWANFAKYGNP
(Bovine)Sbjct  449  FEHRSSKLPWPEWMGVMHGYEIEFVFGLPLERRVNYTKAEEIFSRSIMKRWANFAKYGNP  508

(Human) Query  481  QETQNQSTSWPVFKSTEQKYLTLNTESTRIMTKLRAQQCRFWTSFFPKV  529
                    TQN ST WPVFKS EQKY TLNTES ++ TKLRAQQCRFWT FFPKV
(Bovine)Sbjct  509  NGTQNNSTRWPVFKSNEQKYFTLNTESPKVNTKLRAQQCRFWTLFFPKV  557
```

Figure 12. The Result of the Alignment of the Amino Acid Sequences of Two Enzymes: BchE (Homo Sapiens) and BchE (Bovine serum). The Similarity Parameter for these Enzymes is 91%, and the Coverage Parameter (Blast Query Cover) is 87%.

the initial rates of enzymatic reactions as a function of substrate concentration under steady-state conditions.

Decades of computational and biochemical research have been devoted to studying and understanding the factors that provide enzymes with their exceptional selectivity and high catalytic efficiency. As it is known, enzymes catalyze reactions by binding to a free substrate to form an enzyme-substrate complex. The enzyme stabilizes the transition state of the reaction, allowing the substrate to be more easily converted into product. The resulting enzyme-product complex then dissociates, releasing the product and regenerating the free enzyme, ready for new catalytic cycles. The three-dimensional structure determined by the protein's primary sequence determines the substrate binding site and the enzyme's catalytic center, where the ligands and substrate bind. This typically occurs through weak, reversible, non-covalent electrostatic and van der Waals interactions, although covalent bonds are sometimes used. The restraint put by this structural complementarity allows enzymes to distinguish between substrates and exhibit high specificity both in the reactions they catalyze and in their choice of substrates[57].

In general, the literature notes that the catalytic efficiency of natural enzymes with incomparable substrates can be extremely low; reported k_{cat}/K_m values of only $1M^{-1}\ s^{-1}$ are no exception. In contrast, the average catalytic efficiency (k_{cat}/K_m) of natural enzymes with their related substrates is approximately $10^5M^{-1}\ s^{-1}$, and for some enzymes, approaches $10^9M^{-1}\ s^{-1}$. Thus, the difference between the catalytic efficiency with a related substrate and a dissimilar, unrelated substrate can be several orders of magnitude. The number of natural enzymes that have achieved the maximum possible catalytic efficiency is unknown[58].

For example, by modeling ChEs with the inhibitor donepezil[59] investigators recently demonstrated that

https://doi.org/10.53964/jmab.2026001

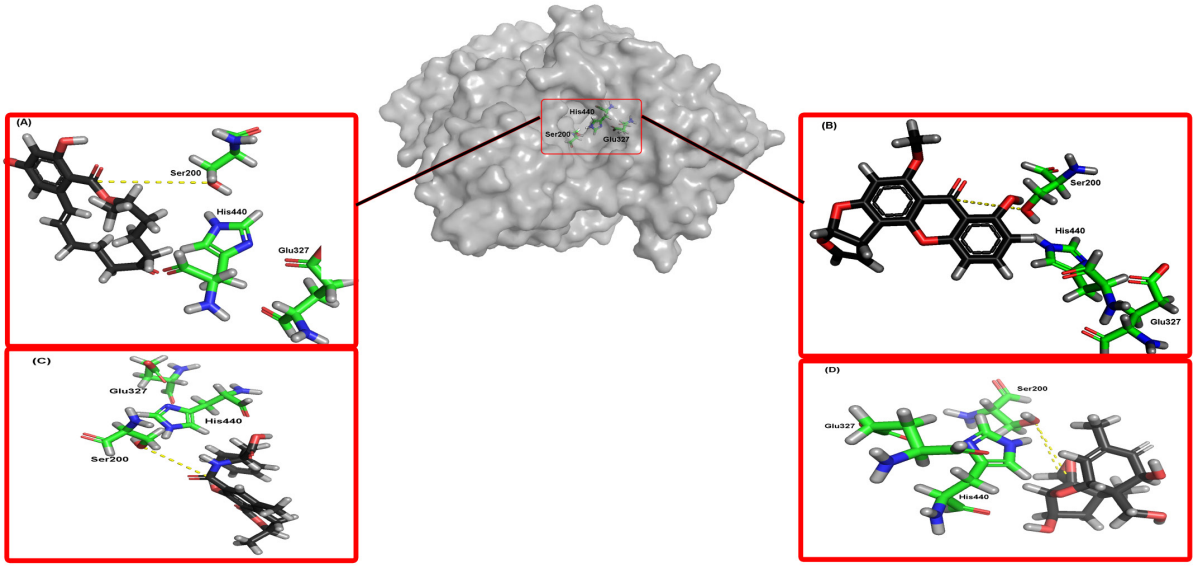


Figure 13. Representation of the Binding of Different Mycotoxins - ZEN (A), STC (B), OTA (C) and DON (D) in the Active Center of the Enzyme AchE using MVGS PyMol.

different volumes of the active site core explain why AchE and BchE have different substrate specificity and catalytic efficiency. Differences in the catalytic sites of enzymes allow selective inhibitors to be designed for them. BchE has various polymorphisms, including inactive forms. In addition to being catalytically active, BchE may interact with other enzymes such as β-amyloid and intracellular neurofibrillary tangles, which are also involved in drug metabolism and detoxification as well as nervous system development.

The study[60] clarifies that the first selectivity domain of ChE, known as the acyl pocket, controls selectivity through differences in the aromatic residues between ChEs. This cluster of aromatic residues is located deep within the active site, where steric hindrance from a pair of phenylalanine residues present in AchE but absent in BchE is the primary difference determining cholinergic selectivity. By constraining the active site in this way, these phenylalanine residues serve to increase the efficiency of acetylthiocholine hydrolysis. The researchers found that replacing these residues in AchE reduces the catalytic efficiency of acetylthiocholine while simultaneously increasing the catalytic efficiency of butyrylthiocholine. The Phe295 residue was found to be the most limiting with respect to butyrylthiocholine hydrolysis, and this amino acid was shown to affect the kinetics of acetylthiocholine hydrolysis by decreasing both the bound turnover number and K_M when replaced by a tyrosine residue. Substitution of bulky aromatic phenylalanine residues with valine and leucine in BchE also allows some ligands to incorporate part of their structure into the acyl pocket of BchE with virtually no overload. The active site cavity of AchE is approximately 200$Å^3$ smaller than that of BchE, and the main reason for such a dramatic difference in the binding site volume is the variability of the acyl pocket residues between BchEs[60].

It is important to keep in mind that there is still no reliable information in the literature about the catalytic efficiency parameters of the 4 mycotoxin molecules used in this study with these two ChEs, excluding the variant with ZEN and the AchE enzyme, which was considered and studied in this study.

Information on the inhibition constants of the inhibitors found and described in a current study for the two enzymes is known and will be described later.

Figures 13 and 14 show the location of molecules of all four studied mycotoxins in the active centers of the AchE and BchE enzymes, respectively.

It can also be said that the lower the binding energy of mycotoxin with enzymes, i.e. the higher the affinity value (kcal/mol), the faster the enzymatic catalysis and the enzymatic hydrolysis process of mycotoxin in the active center of the enzyme, therefore, accordingly, the faster the process of inhibition of these two enzymes AchE and BchE will proceed.

From Table 5 in terms of the high affinity values obtained and the degree of binding in the active center it follows for all four mycotoxin structures, judging by the high values of the obtained binding affinities (kcal/mol), the second BchE enzyme is highly likely to be the most preferable, however, among all four mycotoxins, the highest binding affinity is observed only for the STC mycotoxin during docking with the AchE enzyme.

When comparing the affinity values (kcal/mol) for four different mycotoxins obtained through molecular docking approach with the AchE enzyme, it should be noted that the mycotoxin STC binds most strongly to the active site

https://doi.org/10.53964/jmab.2026001

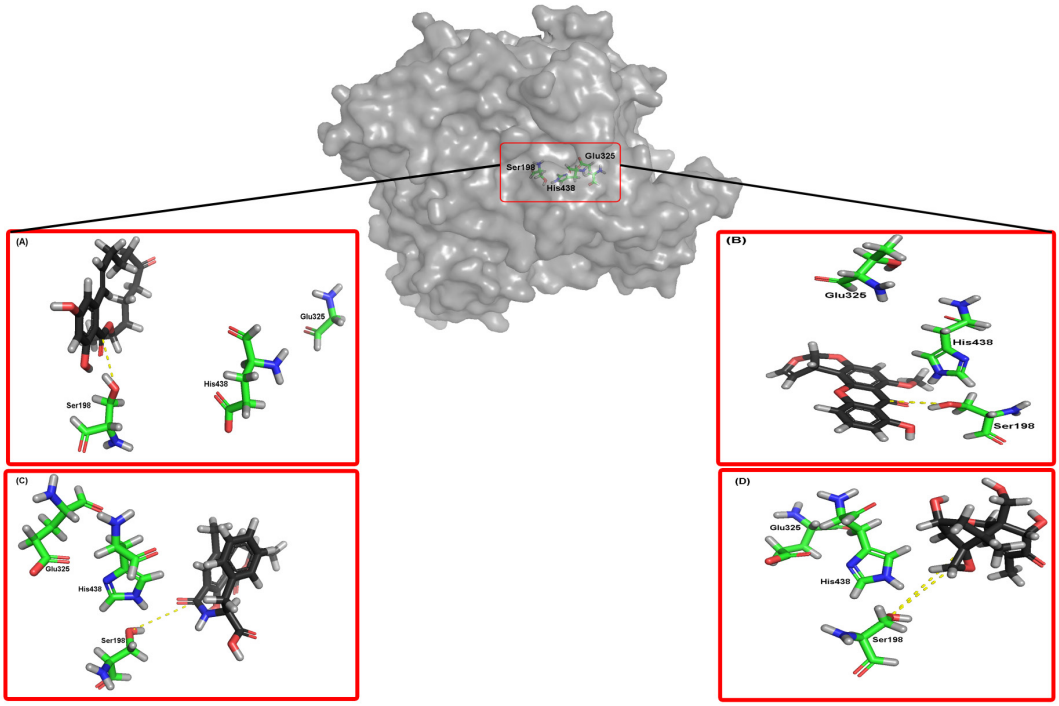


Figure 14. Representation of Binding of Different Mycotoxins - ZEN (A), STC (B), OTA (C) and DON (D) in the Active Center of the Enzyme BchE using MVGS PyMol.

Table 5. Best Results Selected after the Molecular Docking Procedure of Different Mycotoxins - ZEN, STC, OTA and DON and Specific Enzymes Substrates.

	Enzyme AchE	Enzyme BchE
Mycotoxin	Affinity, kcal/mol	Affinity, kcal/mol
ZEN	-7,1	-8,9
STC	-9,8	-9,5
OTA	-5,9	-9,6
DON	-7,4	-7,7
Typical substrate		
Acetylthiocholine	-4,3	
Butrylthiocholine		-4,8

of this enzyme, with an affinity of -9.8kcal/mol. After STC, the highest binding affinity is observed for the mycotoxin DON (-7.4kcal/mol). After the DON molecule, the next mycotoxin, which is highly likely to bind strongly to the AchE enzyme active site, is the mycotoxin ZEN (-7.1kcal/mol). Finally, the last mycotoxin in this series is the one with the weakest potential to bind and inhibit the AchE enzyme, presumably the mycotoxin OTA, with an affinity of -5.9kcal/mol.

Moving on to the case of the BchE enzyme, it is also important to note the result obtained: judging by the values of the affinities obtained during molecular docking, unlike the first AchE enzyme, in this case, the next mycotoxin molecule is OTA, with an affinity of -9.6kcal/mol. After the OTA mycotoxin, STC should be with the affinity value -9,5kcal/mol. ZEN exhibits a higher binding affinity, with a result of -8.9 kcal/mol, compared to the -7.7kcal/mol observed for DON.

According to the above considerations, mycotoxins can be arranged in the following order according to decreasing strength and degree of their binding to the AchE enzyme: STC>DON>ZEN>OTA. For the BchE enzyme, these same mycotoxins can be arranged in the following order: OTA>STC>ZEN>DON.

Comparing the affinities obtained between these two enzymes for the different four mycotoxins, it turns out that the STC mycotoxin is more suitable for the AchE enzyme than the other three mycotoxin molecules, while a nearly identical affinity result is also obtained for OTA mycotoxin in the case of BchE enzyme.

Comparing Tables 2 and 5, which include the results of *in vitro* and *in silico* analyses, we see that the mycotoxin ZEN is most sensitive to the enzyme BchE *in vitro*. Mycotoxin STC maintains this high sensitivity *in silico*, but more sensitive to the enzyme AchE. AchE is the least

sensitive enzyme to the mycotoxin ZEN *in vitro*, while OTA, which binds to the active site of AchE the weakest, is observed *in silico*.

Regarding BchE enzyme, the mycotoxin STC also ranks first in sensitivity to this enzyme *in vitro* on par with the *in silico* results, while mycotoxin OTA, with the highest binding affinity at its active site, outperforms the other three mycotoxin molecules *in silico*. The mycotoxin DON appears to bind weakly to the active site of the enzyme AchE, while *in vitro* the same enzyme appears to be the least sensitive to the mycotoxin OTA.

Also, Table 5 shows that, according to the obtained affinity values (kcal/mol), the affinity of acetylthiocholine in the AchE active site is lower than that of butyrylthiocholine in the BchE active site. This means that, in this case and for the given chosen model and binding position, butyrylthiocholine binds more strongly to the BchE active site than acetylthiocholine in the active site of AchE.

Overall, Table 5 shows that the binding energies (kcal/mol) in the AchE and BchE enzymes active centers for specific substrates are slightly lower than those for the four mycotoxin molecules.

Figures S1-S3 (see Supplementary Information file) show various illustrations of the close proximity of the structures of the mycotoxins OTA, ZEN, DON, and STC, as well as the specific substrates acetylthiocholine (2-acetylsulfanylethyl(trimethyl)azanium) and butyrylthiocholine (2-butanoylsulfanylethyl(trimethyl)azanium) inside the active center of the AchE and BchE enzymes.

The results of the molecular docking of all mycotoxin structures and specific enzyme substrates are presented in Tables S1–S10 in the Supplementary Information file. From these molecular docking results, the best model was selected for each specific case—the binding pose of the mycotoxin and the specific substrate.

The values for the two docked substrate ligands demonstrate the exceptionally high binding energies (kcal/mol) that were obtained as a result of molecular docking for the specific substrates of these two enzymes: binding pose 2 for acetylthiocholine, which has a binding affinity value of -4.3kcal/mol and is close to the catalytic residue Ser200 of approximately 4 Å, with lower and upper Root Mean Square Deviation (RMSD) limits of 2.541Å, 4.337Å, and 2.639Å, 3.597Å, and a higher binding affinity of -4.8kcal/mol in butyrylthiocholine comparison to acetylthiocholine, respectively (see Table 3 and Supplementary Information Tables S1and S2).

The structure of butyrylthiocholine is stabilized by polar hydrogen bonds that arise during polar interactions between its carbonyl group and the NH group of the amino acid residue Gly117 (the distance between the oxygen atom of the carbonyl group of butyrylthiocholine and the hydrogen atom of the NH group of Gly117 is 2.3Å). It should also be noted that the closest proximity of this specific BchE substrate to the catalytic residue Ser198 was also observed in the case of ligand binding pose 2, with a distance of 2Å between the OH group of Ser198 and the oxygen atom of the carbonyl group of butyrylthiocholine.

For the mycotoxin ZEN, this is ligand model binding pose number 5 with the lower and upper RMSD limits of 1.967Å and 4.156Å and has a binding affinity -7.1kcal/mol in the case of enzyme AchE. It should be stated that the structure of the mycotoxin ZEN is stabilized in the active site of the AchE enzyme by additional polar hydrogen bonds, such as the polar interaction between the NH group of the amino acid Gly123 and the oxygen atom of the nearest OH group (distance 3.1Å); and the distance of 2.1Å that occurs between the oxygen atom of the amino acid Gly69 and the hydrogen atom of the same OH group of the mycotoxin ZEN. A similar interpretation can be applied to the amino acids Gly117 and Tyr130, which form and thus stabilize the ZEN molecule via polar hydrogen bonds (the distance between the oxygen atom of the carbonyl group and the hydrogen atom OH of the ZEN group is 2.1Å; the distance between the oxygen atoms of Tyr130 and the oxygen atom of the carbonyl group of ZEN was 2.9Å).

The binding pose number 8 of mycotoxin ZEN in the case of BchE enzyme with the lower and upper RMSD limits of 4.104Å and 4.429Å, has a binding affinity -8.9kcal/mol determined for the enzyme BchE respectively. The molecule of this mycotoxin is stabilized by polar interactions with certain amino acids of the BchE enzyme, located at a maximum distance of 4Å. Among these, one can note the polar contact between the oxygen atom of Tyr332 and the carbonyl group of ZEN (distance 2.9Å). A polar hydrogen bond was observed between the nitrogen atom of the NH group of Gly117 and the oxygen atom of the OH group (the distance was 3.1Å). A similar hydrogen bond with a distance of 3.3Å, arising between the NH group of Gly116 and the carbonyl group of the ZEN structure, also stabilized its molecule. The distances from the hydrogen and oxygen atoms of the OH group of Ser198 to the oxygen atoms of the carbonyl and OH groups in the ZEN structure were 2.2Å and 2.3Å, respectively. The nitrogen atom of the amino acid Ala199 also formed a polar hydrogen bond with the oxygen atom of the OH group at a distance of 3.3Å. It should be noted that the oxygen atom of the carbonyl group of ZEN also forms a polar bond with the hydrogen atom of the NH group of His438 at a distance of 2.6Å.

For the mycotoxin OTA and enzyme AchE, this is ligand model number 9 with the lower and upper RMSD limits of 2.778Å and 3.920Å. The OTA mycotoxin molecule,

specifically in the binding pose of model 9 with binding affinity of -5.9kcal/mol, is located in approximate proximity to one of the residues of the catalytic triad of the AchE enzyme active site, Ser200, at a distance of at most 4 Å between its OH group and the oxygen atom of the OTA carbonyl group. The structure of the OTA mycotoxin in the AchE active site was stabilized by hydrogen bonds. One such polar hydrogen bond is the polar contact between the nitrogen atom of the Gly 119 amino acid and the oxygen atom of the same carbonyl group of the amide bond present in the OTA structure (distance 3.4Å). Polar interactions were also observed with the Tyr130 amino acid, where the distance between the oxygen atom of the OH group of Tyr130 and the oxygen atom of the carboxyl group was 2.8Å.

Binding pose number 8 of mycotoxin OTA ligand for the enzyme BchE with the lower and upper RMSD limits of 3.417Å and 4.954Å was determined. To describe the various types of bonds and interactions that arise with this mycotoxin in the active site of this BchE enzyme, it should be noted that the high affinity of -9.6kcal/mol in the OTA binding position and model number 8 is primarily due to π-π stacking interactions that can occur between the benzene ring of the amino acid Trp82 and one of the benzene rings containing the OH group in the structure. OTA, as both rings are located in a parallel plane relative to each other. In addition, it should be noted that the polar hydrogen bonds between the hydrogen atom of the OH group of the catalytic residue Ser198 and the oxygen atom of the COOH group of OTA with a distance of 2Å, as well as the polar interactions between the NH groups of the amino acids Gly 116 and Gly117 with distances between the corresponding atoms of 2.6 and 2.1Å, also participate in stabilizing the OTA molecule in the active site of BchE. The oxygen atom in the OH group of the COOH group of mycotoxin OTA also forms a polar hydrogen bond with the hydrogen atom of the NH group of the residue of the catalytic triad His438 of the BchE enzyme.

For the mycotoxin DON and AchE enzyme, this is the ligand model number 6 in the case of an enzyme with the lower and upper limit RMSD values of 1.865Å and 3.956Å and binding affinity -7.4kcal/mol. In this case, the DON mycotoxin molecule is stabilized by several polar bonds formed between different atoms within the structure of different amino acid residues and within the DON structure itself. Thus, the oxygen atom of the OH group of the Tyr121 amino acid residue formed two polar contacts with the oxygen atom of the carbonyl group and the hydrogen atom of the methyl group in the DON mycotoxin structure, with distances of 2.9Å and 2.7Å, respectively. A polar hydrogen bond was observed between the oxygen atom of the carbonyl group of the His440 catalytic triad residue and the hydrogen atom of one of the OH groups of DON (distance 2.5Å). The OH group of the Ser200 catalytic residue and the NH group of His440 are also involved in the formation of polar interactions. Thus, the distance between the nitrogen atom of the NH group of His 440 and the oxygen atom of the epoxy group of mycotoxin DON was 3.1Å, and the distance between the hydrogen atom of the OH group of Ser200 and the nearest oxygen atom of the epoxy group of DON was 3.3Å.

Ligand binding pose model 2 in the case of an enzyme BchE with the lower and upper limit values of RMSD 1.387Å and 2.141Å with binding affinity of -7.7kcal/mol was determined.

DON is located at a distance of approximately 4Å from the catalytic residue Ser198 in the BchE active site. One of the OH groups of this mycotoxin is involved in the formation of a polar bond with the oxygen atom of the OH group of the amino acid Tyr332, with the distance between the corresponding hydrogen atoms of the OH group of Ser198 and the oxygen being 2.6Å.

Finally, for the mycotoxin STC, this is the ligand model number 1 in the case of an enzyme with the lower and upper limit RMSD values of 0Å in both cases of the RMSD. The high affinity value of -9.8kcal/mol is explained by the different types of interactions that arise between certain functional groups and atoms in the structure of the STC mycotoxin and certain nearby atoms and functional groups of amino acids. One such important bond is the polar hydrogen bond between the OH hydrogen atom in the STC structure and the carbonyl oxygen atom of the Glu199 amino acid (distance 2.1Å). The structure of this mycotoxin in the ligand-binding position was located at a distance of almost 4Å from the catalytic residue Ser200.

Ligand binding pose model 5 in the case of an enzyme BchE with the lower and upper limit values of RMSD 2.246Å and 3.808Å and at a binding affinity of -9.5kcal/mol was determined.

The amino acids Gly116 and Gly117 participate in the formation of polar hydrogen bonds with the oxygen atom of the carbonyl group in the STC structure. This is facilitated by the close distances shown in the MVGS PyMol measured from the oxygen atom of the carbonyl group of the mycotoxin STC to the hydrogen atoms of the NH groups in the structures of the amino acids Gly116 and Gly117, each of which is 2.5Å. The hydrogen atom of the NH group of the amino acid Gly117 also formed a polar hydrogen bond with the oxygen atom of the CH_2OH group of the mycotoxin STC structure, with a distance of 2.6Å. In the selected model 1 of ligand binding, the mycotoxin STC is located closest to the catalytic residue Ser198, forming a hydrogen bond at a distance of 2Å between the hydrogen atoms of the OH group and the oxygen atom of the carbonyl group of STC.

In the case of the current molecule of the mycotoxin STC, among all 10 obtained and studied mycotoxin ligand binding models in terms of proximity to the catalytic triad Ser198,Glu325, His438 of BchE enzyme, one could also single out model number 6 with lower and higher RMSD bounds of 4.432Å and 5.677Å respectively, and binding affinity of -9.4kcal/mol, where the distance between the hydrogen atom of the OH group of Ser198 and the oxygen atom of the carbonyl group of the mycotoxin STC was 2.2Å (see Supplementary Information Tables S3-S10).

4.2 A Re-docking Validation with Co-crystallized Ligands - Inhibitors

An enzyme inhibitor is a molecule that binds to an enzyme and blocks its activity. Enzymes are proteins that accelerate chemical reactions necessary for life, in which substrate molecules are converted into products. An enzyme facilitates a specific chemical reaction by binding the substrate to its active site, a specialized area on the enzyme that accelerates the most difficult step of the reaction. The inhibitory constant is a type of equilibrium dissociation constant Kd that represents the equilibrium binding affinity for a ligand. The inhibitor constant, Ki, indicates the potency of an inhibitor. K_i represents the concentration at which the inhibitor ligand occupies 50% of the receptor sites in the absence of a competing ligand. The smaller the K_i the greater the binding affinity and the smaller the amount of ligand needed to inhibit the activity of its binding partner.

To confirm the accuracy of the docking setup, repeated docking was verified with co crystallized ligands of both ChEs found and described in the literature. The following chemical compounds were chosen as such co crystallized ligands: 10-(chloroacetyl)-10H-phenothiazine ($C_{14}H_{10}ClNOS$) and 10-(cyclobutylcarbonyl)-10H-phenothiazine ($C_{17}H_{15}NOS$)[61]. For these BchE enzyme inhibitors, the values of the found and calculated inhibition constants have already been described in the literature : 11.02μM and 4.8μM at pH 8.0 and 23°C, respectively. As noted in the literature, the relative potencies of these two inhibitors against both ChEs were 7.3 and 11.6, respectively. In this particular case, these two inhibitors found in the literature are attributed to the enzyme BchE, which was also isolated from *Homo sapiens*. Therefore, molecular docking with these inhibitors in this scientific study was performed only with the enzyme BchE. All molecular structures of the corresponding and suitable inhibitors obtained from BRENDA, the primary enzyme functionality dataset available to the scientific community (www.brenda-enzymes.org).

As a result of the re-docking procedure with the first known natural inhibitor 10-(chloroacetyl)-10H-phenothiazine of both ChEs in the case of the BchE enzyme, it was found that this inhibitor is closest to the active center of BchE in the docking pose of model number 5 with an affinity of -7.4kcal/mol and the lower and upper limits of the RMSD are 2.727Å and 4.857Å, respectively, since with one of the catalytically important residues of the active center Ser198, the distance between the closest atoms is only 2.2Å. This inhibitor is also stabilized in the active center by hydrogen bonds, which are formed with the catalytic residues Ser198 and His438. In addition, it should be borne in mind that as a result of displaying the functions of possible polar bonds with the potential amino acid residues of the BchE enzyme near the inhibitor ligand in MVGS Pymol, it becomes clear that the benzene ring of the inhibitor forms a π–π–π stacking interaction with the benzene ring of the Trp82 residue. Planar aromatic compounds, such as anthracene, triphenylene, and coronene, are exclusively involved in π-π interactions owing to the presence of delocalized π-electrons. This interaction, somewhat stronger than other non-covalent interactions, is a non-covalent interaction between organic compounds containing aromatic components. π-π interactions are caused by the intermolecular overlap of p-orbitals in π-conjugated systems; therefore, they become stronger as the number of π-electrons increases.

A similar π–π stacking contact can also be observed with the amino acid Phe329. An example of this inhibitor's structural stabilization within the enzyme chain is its stabilization due to hydrophobic bonds formed with amino acid residues Tyr120, Gly116, and Gly439. A polar bond was also observed as a result of the contact between the chlorine atom in the inhibitor structure and the nitrogen atom of the Gly117 amino acid residue of the BchE enzyme structure (see Supplementary Information Table S11).

Analyzing the result obtained after molecular docking of the second known inhibitor found in the literature, 10-(cyclobutylcarbonyl)-10H-phenothiazine, it should be noted that its closest location to the active binding site occurs in the very first ligand binding model, which exhibits a high binding affinity (-9 kcal/mol) and zero upper and lower RMSD values compared to the other nine ligand-docking models. In this first binding model, the distance between the hydrogen atom of the catalytic residue Ser198 and the oxygen atom of the carbonyl group of the inhibitor 10-(cyclobutylcarbonyl)-10H-phenothiazine was minimal: 2.2 Å. The inhibitor structure was stabilized by a polar bond between the nitrogen atom of the His438 catalytic residue and the carbonyl group of the inhibitor. When the MVGS PyMol function is included to show residues at a distance of 4 Å from the inhibitor, polar hydrogen bonds between the nitrogen atoms of the Gly115 and Gly117 amino acid residues of the BchE enzyme and the oxygen atom of the inhibitor's carbonyl group also become clearly visible. At a distance of 3 Å from the inhibitor, there was an interaction between the Tyr128 residue and one of the benzene rings of the inhibitor structure. At a distance of 3.5 Å, inhibitor

stabilization is characterized by a hydrophobic interaction between the benzene ring of the Trp82 amino acid residue and one of the benzene rings present in the inhibitor structure (see Supplementary Information Table S12).

The results of molecular docking of the known natural inhibitor 2,2'-(1-(4-bromophenyl)ethane-1,1-diyl) bis(sulfanediyl)diacetic acid ($C_{12}S_2FO_4H_{13}$) at pH 8.0 and 25°C[62] with a known inhibition constant 0.00071μM with respect to the AchE enzyme, it should be noted that of 10 models of the inhibitor's ligand binding poses, only model 3 is suitable in terms of their proximity to the catalytically important residues of the enzyme's active site. Specifically, the inhibitor binds in this pose with an affinity of -7.7kcal/mol, yielding lower and upper bounds of the RMSD of 2.440Å and 2.725Å, respectively. This inhibitor is stabilized in the active site by polar hydrogen bonds formed between the hydrogen atom of the catalytic residue Ser200 and the oxygen atom of the nearby carbonyl group of the ligand structure (distance 3.8Å) and the nitrogen atom of the catalytic residue His440 and the oxygen atom of the hydroxyl group of the inhibitor ligand. A polar contact was also observed between the nitrogen atom of the Gly119 residue and the oxygen atom of the carbonyl group of the inhibitor ligand (see Supplementary Information Table S13).

A well-known natural inhibitor of this AchE enzyme, 2,2'-(1-(4-methoxyphenyl)ethane-1,1-diyl)bis(sulfanediyl) bis(N-(pyridin-2-yl)acetamide) ($C_{23}N_4S_2O_3H_{24}$) at pH 8.0 and 25°C[62] with a known inhibition constant 0.00089μM[36], is closest in its active site to the catalytic triad in the ligand docking pose fifth model. It is important to note that the selected inhibitors were tested and demonstrated their inhibitory activity with the AchE enzyme isolated from *Electrophorus Electricus*.

Thus, according to the results of molecular docking analysis, this inhibitor binds to the active site of the AchE enzyme with a high affinity of -9.5 kcal/mol and lower and upper limits of the RMSD of 1.957 Å and 3.641 Å, respectively. The inhibitor 2,2'-(1-(4-methoxyphenyl) ethane-1,1-diyl)bis(sulfanediyl)bis(N-(pyridin-2-yl) acetamide) is stabilized in the active center of the enzyme due to polar hydrogen bonds between the OH group of Ser200 and the carbonyl group in the structure of the inhibitor ligand (distance 3.9 Å), as well as between the same carbonyl group and the NH group of the catalytic residue His440. Furthermore, similar polar contacts were observed with the Gly119 amino acid residue group after enabling the function to display all amino acid residues adjacent to the inhibitor molecule at a maximum distance of 4 Å. The resulting high affinity value is also associated with additional interactions within the inhibitor structure, one of which is the π- π stacking interaction occurring between the benzene ring of the Tyr334 amino acid residue and one of the benzene rings of the inhibitor molecule, which are located in parallel planes (see Supplementary Information Table S14).

The binding parameter of the active centers of the ChEs used in this study were compared. Among the four known inhibitors of these two enzymes, for which their inhibition constants were described in the literature, the most potent chemical compound exhibiting an inhibitory effect is the inhibitor 2,2'-(1-(4-methoxyphenyl)ethane-1,1-diyl) bis(sulfanediyl)bis(N-(pyridin-2-yl)acetamide) with an obtained affinity value of -9.5 kcal/mol. This compound, by binding more strongly to the active center of AchE, exerts a strong inhibitory effect on AchE compared to 2,2'-(1-(4-bromophenyl)ethane-1,1-diyl)bis(sulfanediyl) diacetic.

Regarding the BchE enzyme, it should be noted that the known inhibitor 10-(cyclobutylcarbonyl)-10H-phenothiazine with an affinity of -9 kcal/mol is superior in binding and inhibition to the active site of the AchE enzyme compared to the inhibitor 10-(chloroacetyl)-10H-phenothiazine.

If we compare the affinity and inhibition constants of the 15 μmol mycotoxin ZEN obtained in the current study and the two mycotoxins presented and described above in the case of AChE with the known values of this inhibition constant, it should be noted that the inhibition constant for ZEN was several times higher than that of these two inhibitors, and the binding affinity value was lower, which for ZEN for a certain selected docking pose was -7.1 kcal/mol, and for the inhibitors 2,2'-(1-(4-bromophenyl) ethane-1,1-diyl)bis(sulfanediyl)diacetic acid and 2,2'-(1-(4-methoxyphenyl)ethane-1,1-diyl)bis(sulfanediyl) bis(N-(pyridin-2-yl)acetamide) - -7.7 kcal/mol and -9.5 kcal/mol, respectively. This also means that when comparing these three inhibitors, including the mycotoxin ZEN, ZEN must be added to the chemical reaction in a larger volume and quantity to inhibit the AchE enzyme than in the case of these two inhibitors.

It should also be stated that repeated re docking was also performed for natural ChE inhibitors such as (+)-(1R,3S,6S)-9-benzyl-3-fluoro 2,4-dioxa-9-aza-3-phosphadecalin 3-oxide[63] in the case of the AchE enzyme and (+/-)-6-bromo-N-((1-(2,3-dihydro-1H-inden-2-yl)-piperidin-3-yl)methyl)-N-(2-methoxyethyl)-2-naphthamide[64] in the case of the BchE enzyme, for which there is no available and known information on calculated inhibition constants in the literature.

In the case of the first inhibitor (+)-(1R,3S,6S)-9-benzyl-3-fluoro 2,4-dioxa-9-aza-3-phosphadecalin 3-oxide ($C_{13}H_{17}FO_2NP$) and the AchE enzyme, its closest arrangement was observed for the first pose of the docking model, that is,

with an affinity of -9.1 kcal/mol and zero values for the lower and upper limits of the RMSD. In this binding pose, the oxygen atom of carbonyl group of this inhibitor is stabilized by polar hydrogen interactions with the hydrogen atom of the hydroxyl group of the catalytic residue Ser200, the distance to which is approximately 4.1 Å, and the hydrogen atom of NH group of the residue His440 with distance 2.7 Å. When all amino acid residues located at a distance of 4 Å from the inhibitor are shown in the MVGS PyMol, the benzene ring in the structure of this inhibitor, due to its position in a parallel plane to the benzene ring of the Tyr334 amino acid, may indicate the occurrence of a π- π stacking interaction between them, which may also contribute to the high affinity resulting from molecular docking (see Supplementary Information Table S15).

When describing the resulting MVGS PyMol image of the inhibitor binding of (+/-)-6-bromo-N-((1-(2,3-dihydro-1H-inden-2-yl)-piperidin-3-yl)methyl)-N-(2-methoxyethyl)-2-naphthamide ($C_{29}H_{33}N_2O_2Br$), it is important to note that of the 10 ligand docking models, only model 3 has the inhibitor conformation closest to the catalytic residues of the BchE enzyme. This is because the inhibitor ligand structure is stabilized by polar bonds formed between the inhibitor's carbonyl group and the OH group of the Ser198 residue (a distance of 2.6 Å), as well as the NH group of the His438 amino acid residue. The high affinity value is -9.4 kcal/mol with the values of the lower and upper limits of the RMSD of 3.590 Å, 4.467 Å, respectively in addition to the existing polar and non-polar contacts, are explained by the π–π stacking interaction, that has arisen between the benzene ring of Tyr332 and one of the benzene rings located parallel to it in the structure of the inhibitor molecule. It should be noted that the pair of benzene rings in the structure of this inhibitor are located almost parallel to each other, which may indicate a possible π–π stacking interaction between these rings (see Supplementary Information Table S16).

Comparing two inhibitors for which inhibition constants are not described in the literature and are unknown, it can be said that the inhibitor (+/-)-6-bromo-N-((1-(2,3-dihydro-1H-inden-2-yl)-piperidin-3-yl)methyl)-N-(2-methoxyethyl)-2-naphthamide binds more strongly to the active site of the BchE enzyme than the inhibitor (+)-(1R,3S,6S)-9-benzyl-3-fluoro 2,4-dioxa-9-aza-3-phosphadecalin 3-oxide) in the active site of AchE.

The Figure 15 below illustrates in general the close proximity and location of all the inhibitors found near the active sites of both ChEs using two different graphical interpretations in MVGS PyMol.

It is a known fact that any RMSD value for a molecular conformational change in the range of 1.5 to 2.0 Å indicates good accuracy of the molecular docking method. In other words, a high-precision molecular docking method typically corresponds to a lower RMSD value for a conformational difference[65].

Numerous examples can be cited among recent scientific studies investigating the effects of AchE or BchE enzymes, representing a promising approach to the development of innovative treatments.

One such study is examining the effects of AchE in essential oils and their bioactive components. This scientific study not only contributes to the understanding of the various molecular mechanisms underlying the biological activity of Lippia origanoides essential oil but also helps develop new natural product-based therapies that meet current demands for creative and viable therapeutic solutions. In a paper[66], the authors also state that Lippia origanoides essential oil demonstrated high inhibitory activity against the AchE enzyme, especially in the nanoformulation, which increases its bioaccessibility and durability. Moreover, the main component, carvacrol, when studied in isolation, also exhibited inhibitory activity against the AchE enzyme, similar to that of the nanoformulation.

Molecular docking analysis showed strong binding affinity between Lippia origanoides essential oil compounds and AchE, confirming its therapeutic potential in neurodegenerative diseases such as Alzheimer's disease[66].

It should be noted that the unforeseen findings of the studies revealed that all the clove oils studied were more effecient as AchE inhibitors than as BchE inhibitors. Moreover, in a study[67], OTA mycotoxin intoxication was connected with metabolic disturbances such as hyperglycemia and hypercortisolemia, but cure with Syzygium aromacum essential oil alleviated these side effects, improved body and brain weight, and restored neurobehavioral functions.

In silico analysis[67] revealed a significant affinity between clove oil and the two studied esterase enzymes AchE and BchE, which was greater than or similar to four neurotransmitters (dopamine, serotonin, norepinephrine, and glutamic acid). These results[67] also highlight the therapeutic potential of clove oils in combating the toxic effects of OTA and pave the way for future research into the mechanisms of action and therapeutic applications of natural compounds for the prevention and treatment of diseases caused by intoxications.

In this study[68], the authors aimed to investigate the neurotoxic potential of four different pesticides: herbicide glyphosate insecticide imazalil, assessing their inhibitory effects on the activities of AchE, BchE, and tyrosinase fungicide), imidacloprid (neonicotinoid insecticide), and lambda-cyhalothrin (pyrethroid using *in vitro* direct

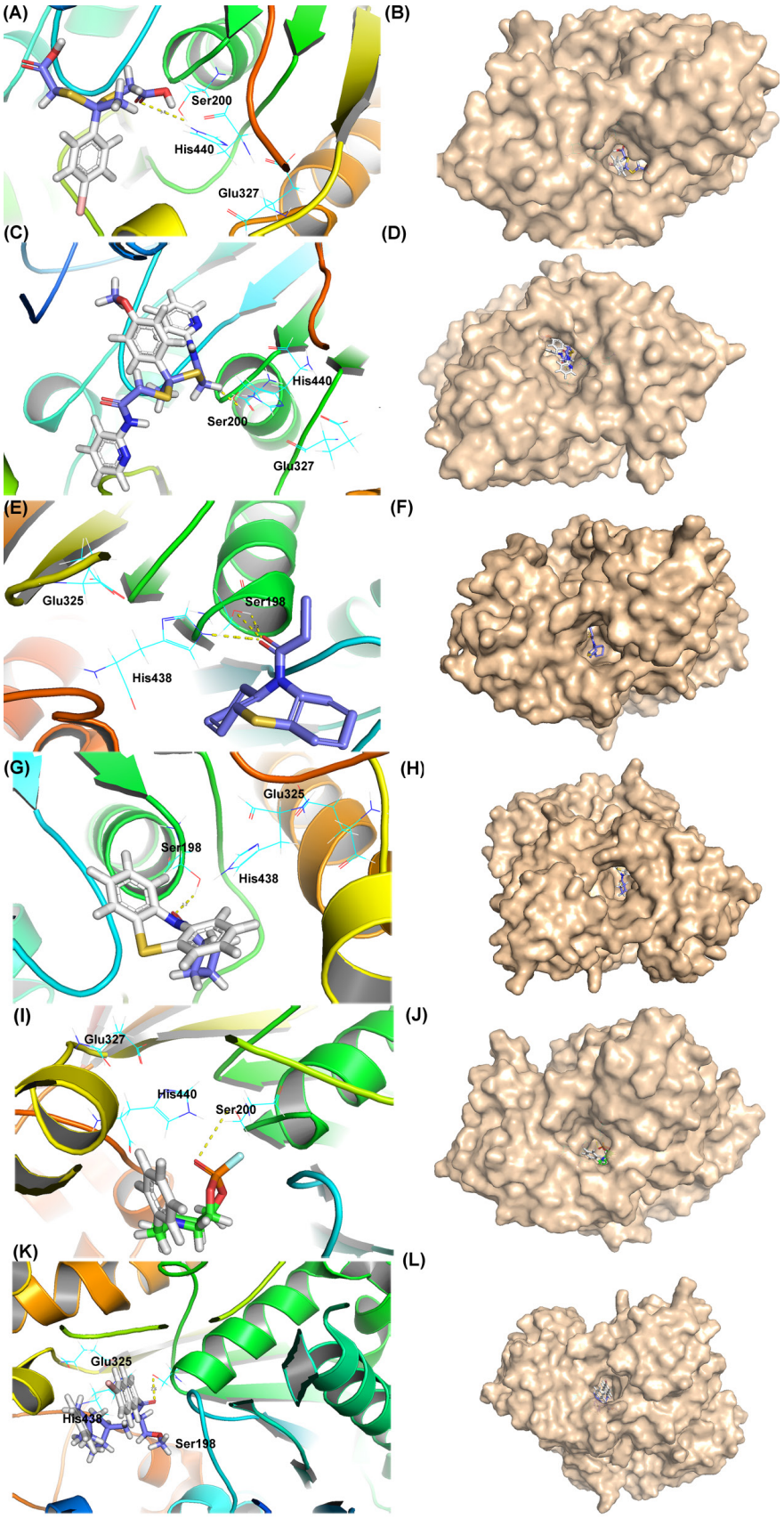


Figure 15. Illustrations of the arrangement of all inhibitor molecules used in the current study in the active sites of AchE and BchE enzymes using PyMol MVGS. Inhibitors 2,2'-(1-(4-bromophenyl)ethane-1,1-diyl)bis(sulfanediyl)diacetic acid (A,B) and 2,2'-(1-(4-methoxyphenyl)ethane-1,1-diyl)bis(sulfanediyl)bis(N-(pyridin-2-yl)acetamide) (C,D) with the AchE enzyme; inhibitors 10-(chloroacetyl)-10H-phenothiazine (E,F) and 10-(cyclobutylcarbonyl)-10H-phenothiazine (G,H) with the enzyme BchE; inhibitors (+)-(1R,3S,6S)-9-benzyl-3-fluoro 2,4-dioxa-9-aza-3-phosphadecalin 3-oxide with the enzyme AchE (I,J) and (+/-)-6-bromo-N-((1-(2,3-dihydro-1H-inden-2-yl)-piperidin-3-yl)methyl)-N-(2-methoxyethyl)-2-naphthamide with the enzyme BchE (K,L). Images B, D, F, H, J, L show two ChEs in spherical representation (oat color), an inhibitor within the active site (purple color) and green color (in case (I) nd (J)).

enzymatic inhibition methods. Imazalil generated dose-dependent inhibition of BchE in the same motif as for AchE enzyme, nevertheless, at lower concentrations (up to 500 μM), imazalil unveiled higher specificity for AchE, and at higher concentrations, the same specificity was found. Imazalil at a concentration of 1 mM inhibited BchE activity by 49±1%. None of the pesticides inhibited tyrosinase activity at concentrations up to 1 mM. After all, it should be noted that the herbicide glyphosate exhibits specificity for AchE but low inhibitory potency. The insecticides imidacloprid and λ-cyhalothrin selectively inhibit AchE, while the fungicide imazalil is a broad-spectr um ChE inhibitor capable of equally inhibiting AchE and BchE. Among these pesticides, the insecticides and fungicide have a higher neurotoxic potential. The insecticides imidacloprid and λ-cyhalothrin selectively inhibit AchE, while the fungicide imazalil is a broad-spectrum ChE inhibitor suitable of equally inhibiting enzymes AchE and BchE.

A recent applications of *in silico* structural bioinformatics methods to enzyme inhibition research are the following. As is well known, computational approaches, specifically molecular docking and molecular dynamics modeling, have appeared as essential tools for the identification and optimization of AchE inhibitors by predicting ligand binding affinity, interaction mechanisms, and conformational dynamics. This work[46] brings a thorough guide for future studies of the AchE enzyme using molecular docking and molecular dynamics modeling procedures. It also summarizes and analyzes studies operated over the past five years and provides a critical assessment of the most widely used computational tools, including AutoDock, AutoDock Vina, and GROMACS, which have significantly contributed to the development of AchE inhibitor screening. Additionally, the authors identified PDB ID 4EY7, the most often used crystal structure of AchE in docking studies, and identified donepezil, a well-established reference molecule widely used as a control in computational screening of new inhibitors.

It can be concluded that the integration of docking and molecular dynamics modeling not only improves hit identification and lead optimization but also provides a deeper understanding of the mechanisms of AchE - ligand interactions, facilitating the rational design of more effective AchE inhibitors[69].

Alzheimer's disease is characterized by advanced cognitive decrease and memory absence and is closely linked to deregulated cholinergic neurotransmission. Since AchE is a critical enzyme in the nervous system responsible for breaking down the neurotransmitter acetylcholine, its inhibition is of significant interest for the treatment of various neurological disorders. Therefore, it is crucial to develop effective AchE inhibitors appropriate of increasing acetylcholine levels, eventually leading to improved cholinergic neurotransmission[70].

The results presented in this study[70] represent a step forward in the development of new thiazoloindazole-based compounds that have the potential to serve as effective AchE inhibitors. Scientific investigations also using molecular docking demonstrated that some of the nitroindazole-based compounds tested surpassed donepezil, a known AchE inhibitor used in the treatment of Alzheimer's disease. Structure–activity relationship analysis revealed that derivatives containing the bis(trifluoromethyl) phenyltriazolyl group exhibit the most promising anti-AchE activity compared to more rigid substituents such as the carbazolyl moiety. The combination of molecular docking and experimental synthesis provides a suitable and promising strategy for the development of new, effective thiazoloindazole-based AchE inhibitors[70].

Flavonoids stand out among natural polyphenolic compounds known for their broad spectrum of biological activity. This study[71] focuses on the inhibitory effect of flavonoids on AchE enzyme and their potential as therapeutic agents for reasonable disorder. It is noted that natural polyphenolic compounds, in particular flavonoids, have established major inhibition of AchE enzyme, situating them as encouraging alternatives or supportives in neuropharmacology.

In vitro, *in vivo*, and *in silico* analyses demonstrate that these flavonoids effectively interact with both the active and peripheral anionic sites of AchE, resulting in increased acetylcholine levels and stabilization of cholinergic signaling. Their mechanisms of action extend beyond simple enzyme inhibition, as they also exhibit antioxidant and antiamyloidogenic properties, thereby offering a multifaceted approach to neuroprotection[71]. Given these results, flavonoids hold significant therapeutic potential as AchE modulators, which has implications for improving cognitive function and treating neurodegenerative diseases. Future research should prioritize enhancing the bioavailability of flavonoids, assessing their efficacy in clinical settings, and exploring their potential synergistic effects in combination with existing treatments to fully realize their potential as neurotherapeutic agents[71].

General antiacetylcholinesterase drugs like galantamine, rivastigmine, donepezil, and tacrine have substantial inhibitory possible[72]. Due to side effects and safety concerns, authors of the study[72] sought to investigate a wide range of phytochemicals and structural analogs of these compounds. Compounds comparable to known drugs and phytochemicals were researched as potential AchE enzyme inhibitors in the cure of Alzheimer's disease.

Foremost virtual screening was accomplished using Pyrx software, which identified 638 molecules with higher

binding affinity compared to the positive controls tacrine (-9.0kcal/mol), donepezil (-7.3kcal/mol), galantamine (-8.3kcal/mol), and rivastigmine (-6.4kcal/mol). Absorption, Distribution, Metabolism, and Excretion (ADME) properties were then assessed, including blood–brain barrier permeability and adherence to Lipinski's five-break rule, resulting in the identification of 88 ADME-tested compounds[72].

BchE enzyme, also acknowledged as pseudocholinesterase and serum ChE, is an isozyme of AchE. It intercedes the degradation of acetylcholine, particularly in pathological conditions[73]. Well-known pharmacological usage of BchE, its mutants, and modulators involve the cure of Alzheimer's disease, multiple sclerosis, cocaine addiction, detoxification in organophosphate poisoning, and monitoring the progression or prognosis of some diseases. This scientific study[73]outlines the selective BchE inhibitors and BchE-related multipurpose ligands published over the past three years, as well as the currently known pharmacological applications of BchE, to understand existing exploration directions. On this matter, some new strategies for developing BchE inhibitors appear intriguing, and modulators based on a mix of histone deacetylase and BchE for the treatment of Alzheimer's disease are extraordinary. Furthermore, BchE's involvement in ghrelin hydrolysis, inhibition of low-density lipoprotein uptake, and reduction of low-density lipoprotein receptor expression suggests its potential to influence lipid metabolism disorders[73].

Few accurate methods exist for detecting acetylcholine. Researchers[74] recently developed a highly sensitive and rapid enzymatic biosensor based on electrospun nanofibers for detecting acetylcholine. This biosensor exploits dual enzymatic reactions involving AchE enzyme and choline oxidase, incapacitated on electrospun nanofibers based on polypyrrole and chitosan.

Electrospun nanofibers acquires a large surface area and high porosity, which improves the sensitivity and selectivity of the biosensor. Structural and morphological analyses, including Scanning Electron Microscopy and Fourier-transform infrared spectroscopy, confirmed the successful synthesis and integration of polypyrrole nanoparticles into chitosan nanofibers. Nanofibers with an average diameter of 280nm were obtained, and electrochemical characterization using cyclic voltammetry and electrochemical impedance spectroscopy demonstrated improved conductivity and efficient enzyme immobilization on nanofiber-modified electrodes. The biosensor[74] established a linear response to acetylcholine concentrations from 10μM to 1mM with a detection limit of 5μM. Selectivity testing disclosed minimal interference from other substances, and stability appraisal confirmed decent operation for 30 days. Application of the biosensor to serum samples spiked with acetylcholine demonstrated accurate detection of acetylcholine, confirming its potential for clinical diagnostics and neurological research.

This innovative approach offers a portable, cost-effective and efficient solution for rapid measurement of acetylcholine, eliminating the limitations of traditional analytical methods[74]. The BchE enzyme is used in the analysis of pesticides, so the high stability and reusability of the enzyme as a result of immobilization processes are important in biotechnological applications[75]. Also by combining enzyme-mediated biological recognition with sensitive transduction mechanisms, such as the cholinesterase-based biosensors used in this study, these biosensors have become necessary and crucial in fields such as food safety, clinical diagnostics, environmental monitoring, pharmaceuticals, agriculture, and biotechnology. Enzyme-based biosensors have evolved into vital tools across a spectrum of applications, including medical diagnostics, environmental monitoring, food safety, biotechnology, and industrial processing.

In agriculture, enzyme-based biosensors facilitate soil and crop health monitoring by detecting agrochemical residues, such as fertilizers and herbicides. Their use supports precision farming practices, enhancing the crop yield while minimizing environmental harm. These sensors enable real-time field diagnostics, providing to more endurable agricultural operations. These type of biosensors, which rely on the catalytic and specific recognition properties of enzymes, are evolving to meet the increasing demand for portable, sensitive, and cost-effective diagnostic and monitoring tools across healthcare, environmental monitoring[76].

5 CONCLUSION

ChEs play an meaningful role in analysis. They can be used as biochemical markers *in vivo* and as biological recognition elements in analytical instruments such as biosensors. Alternatively, the analytical application of ChEs proposes a number of significant advantages. Thus, enzymatic activity is easy to evaluate, and very low detection limits can be attained. Enzyme-based biosensors have emerged as a transformative technology, leveraging the specificity and catalytic efficiency of enzymes across various domains, including medical diagnostics, environmental monitoring, food safety, and industrial processes. They are used for real-time monitoring of food contaminants and quality indicators and facilitate non-invasive monitoring of blood glucose, cholesterol, and biomarkers for various diseases. For environmental monitoring, they are instrumental in detecting pollutants such as pesticides, heavy metals, and endocrine disrupting compounds.

Two different and important methods were used to determine four structurally distinct mycotoxins: the Ellman

spectrophotometric method in an *in vitro* analytical system and an *in silico* approach to describing and interpreting the obtained results using molecular docking analysis.

Based on the calibration curves of inhibition effects of mycotoxins on enzymes, it can be concluded that for the qualitative determination of a mycotoxin by an enzymatic reaction, it is better to use the enzyme with the lower detection limit. Thus, for mycotoxins ZEN and DON, BchE is the preferred enzyme, while for STC, both enzymes are suitable; for mycotoxin OTA - AchE is preferred.

For the quantitative determination of the mycotoxin ZEN, the reaction using BchE is suitable due to its higher sensitivity. STC can be determined by an enzymatic reaction in the presence of both enzymes, AchE and BchE. To determine DON, an enzymatic reaction can only be used in the presence of BchE, since the lower LOD for AchE is twice as high than the LOD (mg/l) for BchE. Mycotoxin OTA can be quantified by both enzymes AchE and BchE, as the operating range of OTA for BchE is within that of AchE, and the maximum working range for AchE is 10 mg/l. In other words,it was found that for the analysis of ZEN it is more expedient to use BchE enzyme, and for the analysis of STC, DON and OTA – AchE. A biosensor based on BchE enzyme is suitable for determining ZEN in low operating ranges, and a biosensor based on AchE enzyme is suitable for ZEN high operating ranges.

Molecular docking, as a powerful tool for predicting the binding structures of potential specific ligands, helped visually identify the locations of the compounds studied in the current study closest to the enzymes' active centers.

To conclude, from the obtained molecular docking results obtained by MVGS PyMol, it should be clarified that, judging by the affinities (kcal/mol), the mycotoxin ZEN is more suitable for the BchE enzyme than for the AchE enzyme, the mycotoxin STC also generally demonstrates greater binding and presumably inhibitory activity with a slight dominance in affinity to the AchE enzyme compared to the case of the BchE enzyme; the mycotoxin OTA demonstrates a lower binding affinity in relation to the AchE enzyme than to the BchE enzyme; and finally, the strongest binding is observed in the active center of BchE for the case of the mycotoxin DON compared to the AchE enzyme variant.

Thus, *in vitro* the inhibitory effects of all four mycotoxins on the activities of AchE and BchE enzymes using the constructed calibration curves, have been demonstrated and proven.

The strong correlation between the docking scores and *in vitro* performance indicates that mycotoxin ZEN may also operate through the mechanism of AchE enzyme inhibition. Competitive inhibition was also demonstrated *in silico* for ZEN,OTA,STC and DON mycotoxin molecules incorporated into the active sites of AchE and BchE enzymes.

Acknowledgements
Not applicable.

Conflicts of Interest
The author declared no conflict of interest.

Data Availability
All data generated or analyzed during this study are included in this published article and its supplementary information files.

Copyright Permissions
Copyright © 2026 The Author(s). Published by Innovation Forever Publishing Group Limited. This open-access article is licensed under a Creative Commons Attribution 4.0 International License (https://creativecommons.org/licenses/by/4.0), which permits unrestricted use, sharing, adaptation, distribution, and reproduction in any medium, provided the original work is properly cited.

Author Contribution
Akhundov R was answerable for the conceptualization, methodology of the research study, and editing of the manuscript, for data analysis, writing and fulfillment of the entire research work.

Abbreviation List
AchE, Acetylcholinesterase
ADME, Absorption, distribution, metabolism, and excretion
BchE, Butyrylcholinesterase
ChE, Cholinesterases
DON, Deoxynivalenol
FTIR, Fourier-transform infrared spectroscopy
LOD, Limit of detection
MVGS, Molecular visualzation and graphics system
OTA, ochratoxin A
RMSD, Root Mean Square Deviation
STC, Sterigmatocystin
ZEN, Zearalenone

References

[1] Jann MW, Shirley KL, Small GW. Clinical Pharmacokinetics and Pharmacodynamics of Cholinesterase Inhibitors. *Clin Pharmacokinet*, 2002; 41: 719-739.[DOI]

[2] Camps P, Muños-Torrero D. Cholinergic Drugs in Pharmacotherapy of Alzheimer's Disease. *Mini-Rev Med Chem*, 2002; 2: 11-25.[DOI]

[3] Gruber-Dorninger C, Müller A, Rosen R. Multi-Mycotoxin Contamination of Aquaculture Feed: A Global Survey. *Toxins*, 2025; 17: 116.[DOI]

[4] Kolawole O, Anusornsak WS, Petchkongkaew A et al.

A systematic review of global occurrence of emerging mycotoxins in crops and animal feeds, and their toxicity in livestock. *Emerg Contam*, 2024; 10: 100305.[DOI]

[5] Sdogati S, Pacini T, Bibi R et al. Co-Occurrence of Aflatoxin B1, Zearalenone and Ochratoxin A in Feed and Feed Materials in Central Italy from 2018 to 2022. Foods, 2024; 13: 313.[DOI]

[6] Giacobini E. Valid Alternative for Therapy of Alzheimer's Disease? *Drugs Aging*, 2001; 18: 891-898.[DOI]

[7] Dave KR, Syal A, Katyare SS. Tissue Cholinesterases. A Comparative Study of Their Kinetic Properties. *Z Naturforsch C*, 2000; 55: 100-108.[DOI]

[8] Pohanka M. Cholinesterases, a target of pharmacology and toxicology. *Biomed Pap*, 2011; 155: 219-229.[DOI]

[9] Vidal JC, Bonel L, Ezquerra A. Electrochemicalaffinity biosensors for detection of mycotoxins: A review. *J Biosens Bioelectron*, 2013; 49: 146-158.[DOI]

[10] Turner NW, Bramhmbhatt H, Szabo-Vezse M et al. Analytical methods for determination of mycotoxins: An update (2009-2014). *Anal Chim Acta*, 2015; 901: 12-33.[DOI]

[11] Brecht A, Gauglitz G. Optical probes and transducers. *Biosens Bioelectron*, 1995; 10: 923-936.[DOI]

[12] Akhundov R, Lyagin I, Senko O et al. Biocatalytic Transformation of Various Mycotoxins: Current Problems and Existing Potential. *IOP Conf Ser Mater Sci Eng*, 2019; 525: 012090.[DOI]

[13] Pohanka M. Cholinesterases in Biorecognition and Biosensors Construction: A Review. *Anal Lett*, 2013; 46: 1849-1868.[DOI]

[14] Andreescu S, Marty JL. Twenty years research in cholinesterase biosensors: From basic research to practical applications. *Biomol Eng*, 2006; 23: 1-15.[DOI]

[15] Pohanka M. Acetylcholinesterase inhibitors: A patent review (2008 - present). *Expert Opin Ther Pat*, 2012; 22: 871-886.[DOI]

[16] Johnson G, Moore SW. The Peripheral Anionic Site of Acetylcholinesterase: Structure, Functions and Potential Role in Rational Drug Design. *Curr Pharm Des*, 2006; 12: 217-225.[DOI]

[17] Cometa F, Lorenzini L, Fortuna S et al. *In vitro* inhibitory effect of aflatoxin B1 on acetylcholinesterase activity in mouse brain. *Toxicology*, 2005; 206: 125-135.[DOI]

[18] Cinthia MM, Spinoza MS, Obregon A et al. Ethidium bromide inhibits rat brain acetylcholinesterase activity *in vitro*. *Chem Biol Interact*, 2006; 162: 121-127.[DOI]

[19] Wong DM, Greenblatt HM, Dvir H et al. Acetylcholinesterase complexed with bivalent ligands related to huperzine A: Experimental evidence for species-dependent protein-ligand complementarity. *J Am Chem Soc*, 2003; 125: 363-373.[DOI]

[20] Saxena A, Redman AMG, Jiang X et al. Differences in active site gorge dimensions of cholinesterases revealed by binding of inhibitors to human butyrylcholinesterase. *Biochemistry*, 1997; 36: 14642-14651.[DOI]

[21] Venkata Krishna PG, Chavali N, Uberbacher E. Flexibility of active-site gorge aromatic residues and non-gorge aromatic residues in acetylcholinesterase. *Chem Pap*, 2013; 67: 300-315.[DOI]

[22] Gilson MK, Straatsma TP, McCammon JA et al. Open "back door" in a molecular dynamics simulation of acetylcholinesterase. *Science*, 1994; 263: 1276-1278.[DOI]

[23] Holtje HD, Kier LB. Nature of anionic or α-site of cholinesterase. *J Pharm Sci*, 1975; 64: 418-420.[DOI]

[24] Ellman GL, Courtney KD, Andres V et al. A new and rapid colorimetric determination of acetylcholinesterase activity. *Biochem Pharmacol*, 1961; 7: 88-95.[DOI]

[25] Chauhan N, Narang J, Pundir CS. Immobilization of rat brain acetylcholinesterase on porous goldnanoparticle-CaCO3 hybrid material modified Au electrode for detection of organophosphorous insecticides. *Int J Biol Macromol*, 2011; 49: 923-929.[DOI]

[26] Amine A, Mohammadi H, Bourais I et al. Enzyme inhibition-based biosensors for food safety and environmental monitoring. *Biosens Bioelectron*, 2006; 21: 1405-1423.[DOI]

[27] Suprun E, Evtugyn G, Budnikov H et al. Acetylcholinesterase sensor based on screen-printed carbon electrode modified with prussian blue. *Anal Bioanal Chem*, 2005; 383: 597-604.[DOI]

[28] Masson P, Lockridge O. Butyrylcholinesterase for protection from organophosphorus poisons: Catalytic complexities and hysteretic behavior. *Arch Biochem Biophys*, 2010; 494: 107-120.[DOI]

[29] Harel M, Sussman JL, Krejci E et al. Conversion of acetylcholinesterase to butyrylcholinesterase: modeling and mutagenesis. *Proc Natl Acad Sci USA*, 1992; 89: 10827-10831.[DOI]

[30] Adler M, Filbert MG. Role of butyrylcholinesterase in canine tracheal smooth-muscle function. *FEBS Lett*, 1990; 267: 107-110.[DOI]

[31] Agu PC, Afukwa CA, Orji OU et al. Molecular docking as a tool for the discovery of molecular targets of nutraceuticals in diseases management. *Sci Rep*, 2023; 13: 13398.[DOI]

[32] Kerwin SM. ChemBioOffice Ultra 2010 Suite. *J Am Chem Soc*, 2010; 132: 2466-2467.[DOI]

[33] Morris GM, Huey R, Lindstrom W et al. AutoDock4 and AutoDockTools4: Automated docking with selective receptor flexibility. *J Comput Chem*, 2009; 30: 2785-2791.[DOI]

[34] Trott O, Olson AJ. AutoDock Vina: Improving the speed and accuracy of docking with a new scoring function, efficient optimization, and multithreading. *J Comput Chem*, 2010; 31: 455-461.[DOI]

[35] Tang S, Chen R, Lin M et al. Accelerating AutoDock Vina with GPUs. *Molecules*, 2022; 27: 3041.[DOI]

[36] Röhrig UF, Goullieux M, Perez MAS et al. SwissDock: major enhancements for small-molecule docking with Attracting Cavities and AutoDock Vina. *Nucleic Acids Res*, 2024; 52: W324-W332.[DOI]

[37] Buccheri R, Rescifina A. High-Throughput, High-Quality: Benchmarking GNINA and AutoDock Vina for Precision Virtual Screening Workflow. *Molecules*, 2025; 30: 3361.[DOI]

[38] Baker NA, Sept D, Joseph S et al. Electrostatics of nanosystems: Application to microtubules and the ribosome. *Proc Natl Acad Sci USA*, 2001; 98: 10037-10041.[DOI]

[39] Dolinsky TJ, Czodrowski P, Li H et al. PDB2PQR: expanding and upgrading automated preparation of biomolecular structures for molecular simulations. *Nucleic Acids Res*, 2007; 35: W522-W525.[DOI]

[40] Odhar HA, Hashim AF, Humadi SS et al. Ligand-based virtual screening of FDA-approved drugs to identify new inhibitors against lactate dehydrogenase enzyme of malaria parasites. *Int J Appl Pharm*, 2024; 16: 15-21.[DOI]

[41] Kumar SP. Molecular Docking Analysis of Haloperidol Binding to the D2 Dopamine Receptor Using AutoDock Vine and PyMOL. *ChemRxiv*, 2025.[DOI]

[42] Akhundov R. Evaluation and Comparison of the Feasibility of Enzymatic Hydrolysis of Specific Mycotoxin Structures in the Active Sites of CPA and CbhA Enzymes using Molecular Docking Analysis and Molecular Visualization Graphic Tools. *J Mod Biol Drug Discov*, 2025; 4: 5.[DOI]

[43] Galdino GT, DesCoteaux T, Teruel N et al. NRG Suite-Qt: a PyMOL plugin for high-throughput virtual screening, molecular docking, normal-mode analysis, the study of molecular interactions, and the detection of binding-site similarities. *Bioinformatics Adv*, 2025; 5: vbaf129.[DOI]

[44] Nivatya HK, Singh A, Kumar N. Assessing molecular docking tools: understanding drug discovery and design. *Futur J Pharm Sci*, 2025; 11: 111.[DOI]

[45] Zhang Y, Yang L, Zhang Q et al. The molecular mechanisms through which psilocybin prevents suicide: evidence from network pharmacology and molecular docking analyses. *Transl Psychiatry*, 2025; 15: 202.[DOI]

[46] Ponnaganti S. Computational Insights into the Binding Mechanism of L6I with Keap1 Kelch Domain (5FNU): A Molecular Docking Approach. *ChemRxiv*, 2025.[DOI]

[47] Selvam AA, Bandral SK, Pavadai P et al. Computational identification and molecular characterization of novel Aurora-B kinase inhibitors: Pharmacophore modeling, docking, and molecular dynamics simulations. *Inn Med Oncol*, 2025.[DOI]

[48] Jadhav S, Dighe PR, Kumbhare MR. Synthesis, *In Vitro* Evaluation, and Molecular Docking Studies of Novel Pyrazoline Derivatives as Promising Bioactive Molecules. *J Pharm Sci Comput Chem*, 2025; 1: 1-11.[DOI]

[49] Novales NA, Schwans JP. Comparing the effects of organic cosolvents on acetylcholinesterase and butyrylcholinesterase activity. *Anal Biochem*, 2022; 654: 114796.[DOI]

[50] Baswar D, Mishra A. Effect of Organic Solvents on Acetylcholinesterase Inhibition and Enzyme Kinetics. *Cent Nerv Syst Agents Med Chem*, 2023; 23: 40-47.[DOI]

[51] Copeland RA. Enzymes (second edition). A practical introduction to Structure, Mechanism, and Data Analysis. Wiley-VCH: Weinheim, Germany, 2000.[DOI]

[52] Gegenschatz SA, Chiappini FA, Tavares CT et al. Binding the gap between experiments, statistics, and method comparison: A tutorial for computing limits of detection and quantification in univariate calibration for complex samples. *Anal Chim Acta*, 2022; 1209: 339342.[DOI]

[53] Leite M, Freitas A, Barbosa J et al. Comprehensive assessment of different extraction methodologies for optimization and validation of an analytical multi-method for determination of emerging and regulated mycotoxins in maize by UHPLC-MS/MS. *Food Chem Adv*, 2023; 2: 100145.[DOI]

[54] Mello FV, Pereira C, Özkan B et al. Toxicological Responses of Juvenile Gilthead Seabream to Enniatin B and Fumonisin B1. *Int J Mol Sci*, 2025; 26: 5676.[DOI]

[55] Dafferner AJ, Lushchekina S, Masson P et al. Characterization of butyrylcholinesterase in bovine serum. *Chem Biol Interact*, 2017; 266: 17-27.[DOI]

[56] Sinko G, Kovarik Z, Reiner E et al. Mechanism of stereoselective interaction between butyrylcholinesterase and ethopropazine enantiomers. *Biochimie*, 2011; 93: 1797-1807.[DOI]

[57] Borkakoti N, Ribeiro AJM, Thornton JM. A structural perspective on enzymes and their catalytic mechanisms. Curr Opin Struct Biol, 2025; 92: 103040.[DOI]

[58] Goldsmith M, Tawfik DS. Enzyme engineering: reaching the maximal catalytic efficiency peak. *Curr Opin Struct Biol*, 2017; 47: 140-150.[DOI]

[59] Ortega de Oliveira PC, Matias da Silva G, Cass QB et al. Natural products as a source of cholinesterase inhibitors. *Pharmacol Res Nat Prod*, 2024; 5: 100099.[DOI]

[60] Michael D, Wang GY, Pang J. The Selectivity of Butyrylcholinesterase Inhibitors Revisited. *Molecules*, 2025; 30: 4201.[DOI]

[61] Masson P, Xie W, Froment MT et al. Effects of mutations of active site residues and amino acids interacting with the Omega loop on substrate activation of butyrylcholinesterase. *Biochim Biophys Acta*, 2001; 1544: 166-176.[DOI]

[62] Darvesh S, McDonald RS, Penwell A et al. Structure-activity relationships for *inhibition of human cholinesterases by alkyl amide phenothiazine derivatives. Bioorg Med Chem*, 2005; 13: 211-222.[DOI]

[63] Simon S, Massoulié J. Cloning and expression of acetylcholinesterase from Electrophorus. Splicing pattern of the 3' exons in vivo and in transfected mammalian cells. *J Biol Chem*, 1997; 272: 33045-33055.[DOI]

[64] Lorenzetto P, Wächter M, Rüedi P. Synthesis and characterization of enantiomerically pure cis- and trans-3-fluoro-2,4-dioxa-9-aza-3-phosphadecalin 3-oxides as acetylcholine mimetics and inhibitors of acetylcholinesterase. *Helv Chim Acta*, 2012; 95: 746-767.[DOI]

[65] Kosak U, Brus B, Knez D et al. The magic of crystal structure-based inhibitor optimization: development of a butyrylcholinesterase inhibitor with picomolar affinity and in vivo activity. *J Med Chem*, 2018; 61: 119-139.[DOI]

[66] Júnior QS, Rodrigues QS, Barroso AS et al. Essential Oil of Lippia origanoides Kunth: Nanoformulation, Anticholinesterase Activity, and Molecular Docking. *Molecules*, 2025; 30: 1554.[DOI]

[67] Brahmi M, Adli DEH, Kaoudj I et al. Chemical Composition, In Vivo, and *In Silico* Molecular Docking Studies of the Effect of Syzygium aromaticum (Clove) Essential Oil on Ochratoxin A-Induced Acute Neurotoxicity. *Plants*, 2025; 14: 130.[DOI]

[68] Martins-Gomes C, Tiago EC, Silva TL et al. Neurotoxicity Assessment of Four Different Pesticides Using *In Vitro* Enzymatic Inhibition Assays. *Toxics*, 2022; 10: 448.[DOI]

[69] Reynoso-García MF, Nicolás-Álvarez DE, Tenorio-Barajas AY et al. Structural Bioinformatics Applied to Acetylcholinesterase Enzyme Inhibition. *Int J Mol Sci*, 2025; 26: 3781.[DOI]

[70] Laghchioua FE, da Silva CFM, Diana CGA et al. Design of Promising Thiazoloindazole-Based Acetylcholinesterase

Inhibitors Guided by Molecular Docking and Experimental Insights. *ACS Chem Neurosci*, 2024; 15: 2853-2869.[DOI]

[71] Cichon N, Grabowska W, Gorniak L et al. Mechanistic and Therapeutic Insights into Flavonoid-Based Inhibition of Acetylcholinesterase: Implications for Neurodegenerative Diseases. *Nutrients*, 2025; 17: 78.[DOI]

[72] Azmal M, Sahadot HM, Naimul HSM et al. A computational approach to identify phytochemicals as potential inhibitor of acetylcholinesterase: Molecular docking, ADME profiling and molecular dynamics simulations. *PLoS One*, 2024; 19: e0304490.[DOI]

[73] Harakandi H, Wang L, Guo H. New insights into butyrylcholinesterase: Pharmaceutical applications, selective inhibitors and multitarget-directed ligands. *Eur J Med Chem*, 2024; 275: 116569.[DOI]

[74] Yildirim N, Akkoyun TS, Umut H et al. Development of a Polypyrrole-Chitosan Electrospun Nanofiber-Based Enzymatic Biosensor for Sensitive and Rapid Detection of Acetylcholine. *ACS Appl Polym Mater*, 2025; 7: 611-621.[DOI]

[75] Necip A. Immobilization of butyrylcholinesterase on chitosan/chitosan-TiO2 via glutaraldehyde cross-linking: enzyme stability, reusability and characterization. *Chem Pap*, 2025; 79: 6365-6373.[DOI]

[76] Sonowal K, Borthakur PP, Pathak K. Advances in Enzyme-Based Biosensors: Emerging Trends and Applications. *Eng Proc*, 2025; 106: 5.[DOI]